UNIVERSITY OF CALIFORNIA
SANTA CRUZ

MODELING THE HUMAN KNEE USING TENSEGRITY

A thesis submitted in partial satisfaction of the
requirements for the degree of

Master of Science

in

COMPUTER ENGINEERING
with an emphasis in ROBOTICS AND CONTROL

by

Dennis Castro

March 2017

The thesis of Dennis Castro
is approved:

Professor Mircea Teodorescu, Chair

Professor Sri Kurniawan

Professor Donald Wiberg

Dean Tyrus Miller
Vice Provost and Dean of Graduate Studies

Table of Contents

List of Figures

List of Tables

Abstract

Modeling the Human Knee using Tensegrity

by

Dennis Castro

This thesis presents a preliminary investigation of using the principles of tensegrity to model the interactions that make up the human knee. The main theory behind tensegrity is to suspend compressionable members in a network for tensile members. Current robotics literature views the human knee as a revolute joint or as a ball and socket joint. Although the simplicity of this approach has significant advantages for robotic systems, this approach has significant disadvantages for biologically inspired systems (e.g., prosthetics). The current research will investigate if tensegrity based robotic design could be used for the next generation robotics and prosthetic devices.

Acknowledgments

The author would like to thank the University of California, Santa Cruz's Center for Information Technology Research in the Interest of Society (CITRIS) for their continued support. I would like to thank my committee for spending their precious time reviewing this document and providing me guidance. I would like to specifically thank professor Mircea Teodorescu, my advisor, for providing 2 years of guidance and insight in my research career. Also, Steve Lessard, Dawn Hustig, and my team of undergraduates, Erik Jung, Victoria Ly, Gilbert Barrios, Anil Celik, and Deepak Sherma for providing support and feedback and helping me with physical and computer modeling. Lastly the author would like to thank his wife, Beverly Castro, and his daughter, Amelia Castro.

Chapter 1

Introduction

1.1 Motivation

Knee injuries present one of the highest clinical and public health injury related burdens, given the high incidence of knee injuries across the age continuum and the frequent need for surgical repair and long-term rehabilitation [1]. The knee is the most commonly injured joint by adolescent athletes, with an estimated 2.5 million sports-related injuries presenting to EDs [emergent departments] annually [2, 3]. It is my belief that by applying a different train of thought on how the knee joint works we would be able to mitigate knee injuries and help future rehabilitation efforts determine appropriate methods that will not only speed up the recovery time but educate those on ways to prevent knee injuries. This type of knowledge may also help expand our designs on robotics, prosthetic, and enhancement devices.

Our current models of the knee joint stems from the traditional method of

simplifying complex systems into simpler systems for analysis. For example the knee joint is currently modeled as a hinge joint that is constrained by the muscles surrounding it, see Figure 1.1.

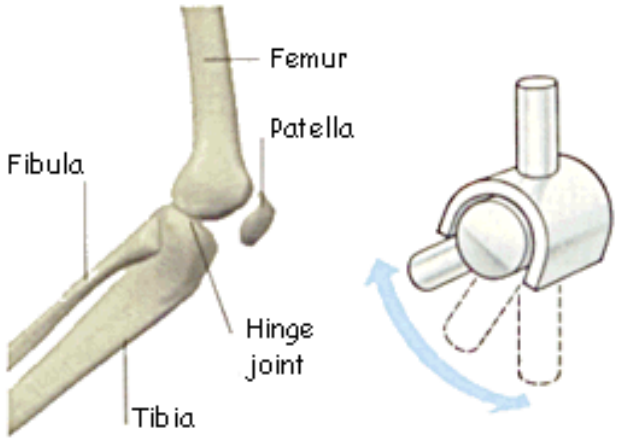

Figure 1.1: Knee Joint Representation [9]

This type of representation has limited our thinking that the joints interact as a low friction hinge joint with the femur and tibia interaction at the head with cartilage cushioned between them. This has been our understanding for a while now and has been associated with conditions like arthritis and chronic joint pains. With the wear and tear of the cartilage the joints grind together and cause inflammation or tearing. But what if the cartilage isn't the only structure that is holding the bones apart at the joint? What if our modeling of these joints are wrong? Reasons why this is important span from the understanding of how our bodies move to the applied research on exoskeleton models that better help the patience/person perform functions. Some of the opportunities that I have found are:

- Robot-Human interaction in industry. Current robots in the industry (automotive and fabrication) are large and powerful, making it dangerous to work around. Thus, soft robotics/light weight robots would help make this interaction safe.

- Current passive leg prosthetic don't provide the stability and "natural" gait that end-users wanting. Would be interesting to led research in the direction of a "lightweight" leg prosthesis (both passive and active). Current rigid passive design are like the transfemoral prosthesis from Vanderbilt [14]

- By understanding the musculoskeletal impact of the major muscle groups on the function of the knee (from a tensegrity prospective), an improved brace or exoskeleton could be used to rehabilitate and/or support the knee joint.

1.2 Previous Work

To gain a better grasp on the project as a whole an understand of what Tensegrity is and how it has been applied is needed. In addition to this, background on how current technologies try to mimic or recreate the knee joint would help to present some of the uses of this work.

1.2.1 Lower Limb Biomimicry Robotics and Exoskeleton

Currently there has been progress with the development of humanoid robots like the Asimo (Honda)[18] and the KHR-3 (KAIST)[19], Figure 1.2, which rely on hinge joints or plain axis rotational joints for the knee joint, but the human knee joint "is a

rolling and sliding joint not a plain axis rotation joint",[10]. Even though these systems have their advantages such as simplification of a complex system, well understood force analysis, and linear force analysis, there are also disadvantages. Limitation to these classical robot designs have been relatively expensive, heavy, and bulky. Particularly, high ratio reduction gears, have been a continuous limitation to low-cost robot designs", [11].

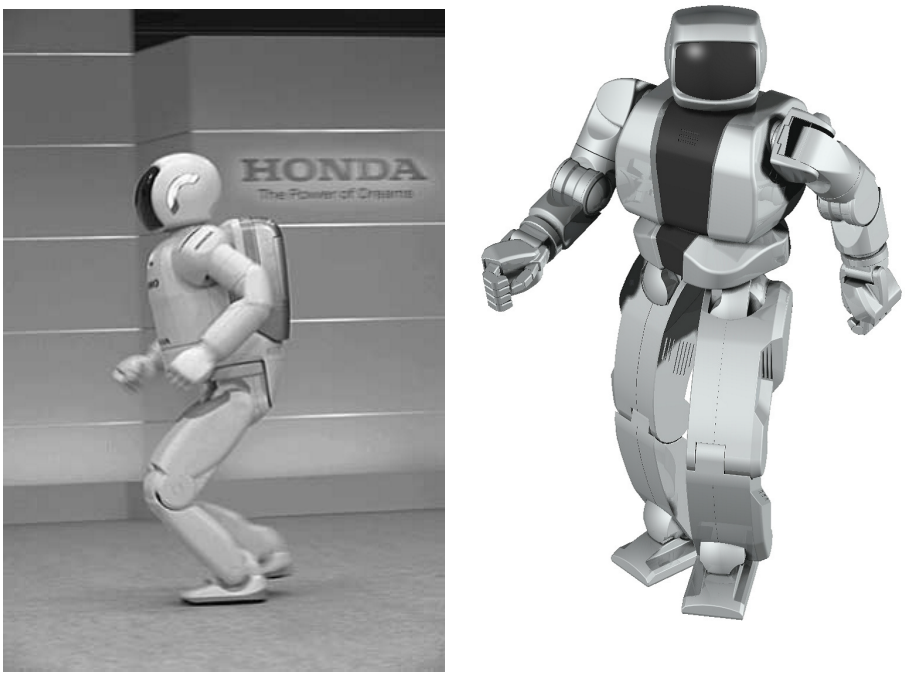

(a) Honda ASIMO [18] (b) KAIST KHR-3 [19]

Figure 1.2: Humanoid Robots

It seems with our understanding of human anatomy and development of better technology we have started creating robots that are more in-line with anatomically correct motions. Currently the field of Soft Robots and Cable Driven Actuators have

been making great strides forward in humanoid robots and beyond (exoskeleton, automation, etc.). As seen in Figure 1.3, this design of the knee joint is directly inspired by the anatomically correct joint. By using cable driven actuation and a type of patella this robot is able to move its knee in a way that mimics the human knee.

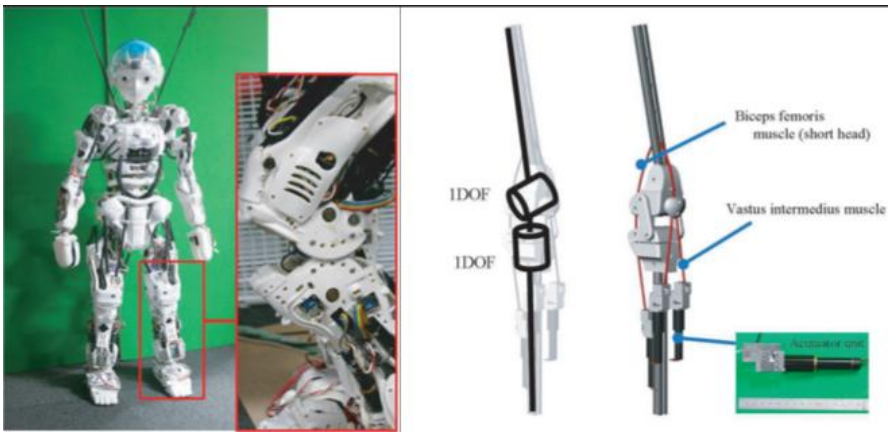

Figure 1.3: Knee Joint of Kojiro from the University of Tokyo, [11]

1.2.2 Tensegrity

To better understand the suggested type of modeling, the definition of tensegrity is needed. Tensegrity is a structural principle based on the use of isolated components in compression inside a net of continuous tension, in such a way that the compressed members (usually bars or struts) do not touch each other and the prestressed tensioned members (usually cables or tendons) delineate the system spatially [6]. This type of modeling suggests that the muscles around the joint help support the joint by pulling the upper and lower leg away from each other. Theoretically this means that some of the conditions like arthritis and other joint pains could be mitigated by

strengthening the muscles around the joint.

Dr. Stephen M. Levin, an Orthopedic Surgeon, has discussed his ideas on how the human body, specifically the fascia, supports and shapes the body. Through this work he has focused on an area of biotensegrity. Biotensegrity reverses the centuries old concept that the skeleton is the frame upon which the soft tissue is draped, and replaces it with an integrated fascial fabric with floating compression elements, (bones in vertebrates), enmeshed within the interstices of the tensioned elements[4].

Referring to Figure 1.4, Dr. Levin stated "It is obvious that lever systems, the standard for over three centuries, does not match the qualities needed for biologic modeling, and tensegrity icosahedral systems are a perfect match [4].

Biologic Systems	**Lever Systems**	**Tensegrity Icosahedron**
Nonlinear	*Linear*	Nonlinear
Global	*Local*	Global
Structurally Continuous	*Discontinuous*	Structurally Continuous
Gravity Independent	*Gravity Dependent*	Gravity Independent
Omnidirectional	*Unidirectional*	Omnidirectional
Low Energy	*High Energy*	Low Energy
Flexible Joints	*Rigid Joints*	Flexible Joints

Figure 1.4: Modeling comparison for Biologic System [4]

Tom Flemons is an inventor that has used tensegrity as a base to make static models that resemble the human anatomy. Inspired by his Leg Model, Figure 1.5, a design was created for the knee joint. This is a simplified model of knee as it does not include the patella and how it interacts in the knee model, but follows the general concept of tensegrity. As seen from his work, this model is a static structure that is made up of wood and bungee cord. When force is applied to the model the structure

starts to mimic flexion at the knee and dorsiflexion at the ankle joint.

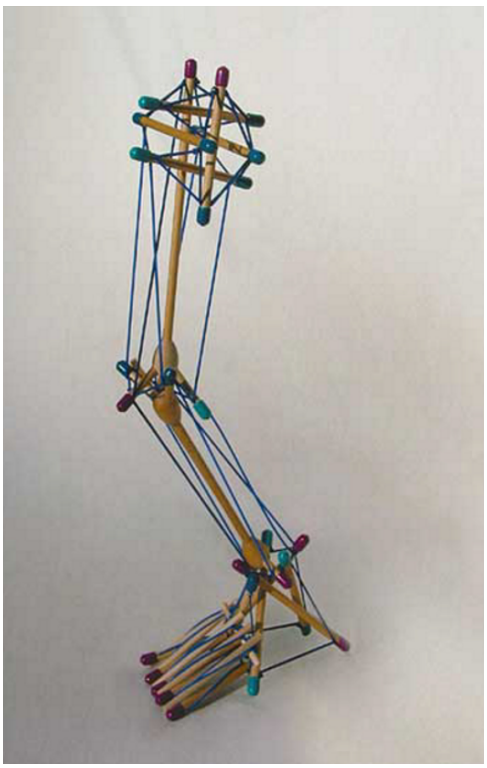

Figure 1.5: Tom Flemons Leg Model [7]

1.2.3 Tensegrity and Biotensegrity Robotics

At the University of California Santa Cruz (UCSC), in conjunction with NASA Ames Research Center, there has been research to investigate how tensegrity structures can be applied to space exploration and modeling the human arm.

SUPERball, the Spherical Underactuated Planetary Exploration Robot Ball, is a distributed robotic system design prototype in active development at the Dynamic Tensegrity Robotics Lab (DTRL) at NASA Ames Research Center [13]. This tensegrity

structure consists of a 6-bar icosahedron with 24 tension cables. This project is aimed for a new type of exploration robots that has a high strength-to-weight ratio and ability to deploy from compact configurations. The SUPERball was designed to perform like current rovers while suspending payload or scientific equipment in the center of the tensegrity structure.

Figure 1.6: SUPERball [13]

A bio-inspired tensegrity structure of the human arm has been worked on by UCSC PhD candidate, Steven Lessard. His work has gone through the structural design of a tensegrity elbow joint design by Dr. Graham Scarr and building a model to verify the movement [16]. From here he has included various designs for a shoulder joint using a simulation program (NTRT) [17].

In addition to this work physical models were created to verify the simulations, Figure 1.8. These models mimicked the flexion of the elbow, extension of the shoulder, and shoulder lift. From the figure it can be seen that the model was created using dowels and different type of elastic elements.

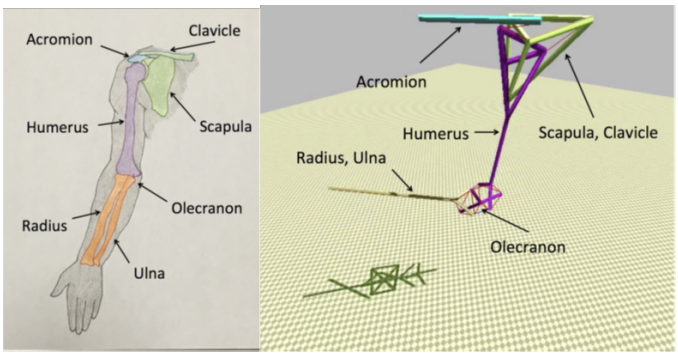

Figure 1.7: Bio-inspired tensegrity manipulator simulation comparison [15]

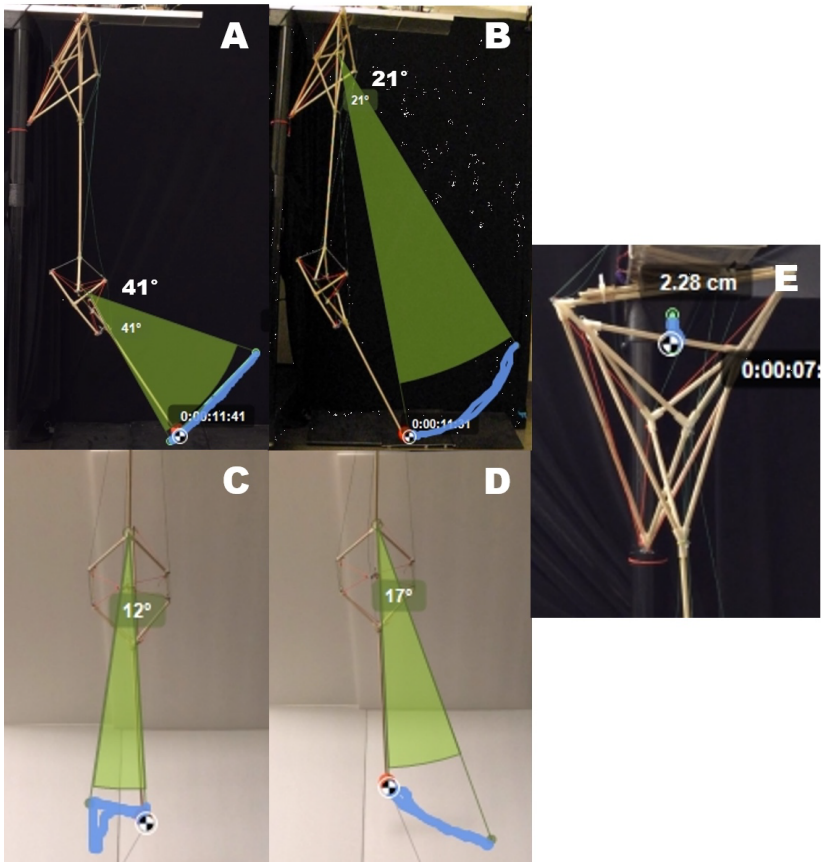

Figure 1.8: (a) Tetrahedrons: A: Shoulder Pitch, B: Elbow Pitch, C: Right Yaw, D: Left Yaw, E: Shoulder Lift [15]

1.3 Approach

For my project I would like to create a model of the knee joint as a tensegrity structure. To do so I will have to implement this in a software that will be able to simulate and model this tensegrity structure. Currently the most promising software is the NASA Tensegrity Robotics Toolkit (NTRT), which has been used to model their current tensegrity robots and create the controllers to move these structures [12]. Some of the big picture goals of this project are as followed:

- Deeper understanding of the interaction of the musculoskeletal and skeletal system (all animals)
- Provide insight in appropriate rehabilitation methods
- Create new low energy, omni-directional, and structurally continuous robots
- Developing new rehabilitation devices
- Lightweight wearable devices

My approach is more of a design evolution on creating a tensegrity/ biotensegrity/ bio-inspired knee joint that mimics knee flexion and extension. This would include simulation of the tensegrity structures in NTRT, determining the correct tension elements/muscle groups to activate to make the structure perform flexion/extension, compare tensegrity models to classical model (hinge joint), and finally the creation of a physical model.

Chapter 2

Simulation and Design

To understand and compare the classical joints to a tensegrity model we first had to make equivalent models in NTRT and Matlab of a knee joint. NTRT (NASA Tensegrity Robotics ToolKit) is a collection of C++ and MATLAB software modules for the modeling, simulation, and control of Tensegrity Robots, [12]. These models would need to simulate the full 160 Degrees of flexion, just as the human knee can do [23].

2.1 Matlab

For the Matlab portion of this project a simple joint was created using the double pendulum example in Matlab. As seen in Figure 2.1 the model is equivalent to a simple hinge joint. To get only knee flexion the upper bar was wielded in place to ensure only the lower bar would be able to move. Once the model was completed a controller was made to actuate the joint to a certain point. Both displacement and forces were monitored and graphed for this model. Due to the nature of this hinge joint

the displacement of the end effector could only be seen in the Y and Z coordinate plane.

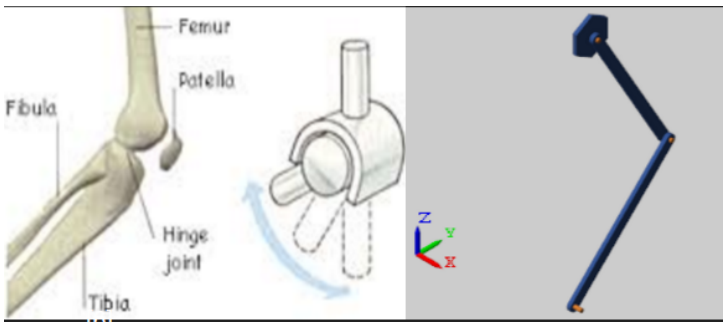

Figure 2.1: Matlab Knee Joint Comparison to Hinge Joint[9]

2.2 NTRT

For the NTRT simulations the models were based off the passive tensegrity structure created by Tom Flemons, see Figure 1.5. From his structure we only focused on the knee joint. A better representation can be seen in Figure 2.2. Within NTRT the model was built then a simplified controller was created to active a muscle group to cause flexion. In addition to this a marker was added to determine the displacement of the end effector in the X,Y,and Z coordinate plane.

2.2.1 Model Iteration

The first model design was of the simple geometry that was built off of the 3-prism example file in NTRT example list. This model did not contain the correct geometry from Tom Flemons' model but was a test model to see the muscle placements and the affects of environment changes such as density, gravity, pretension, and model

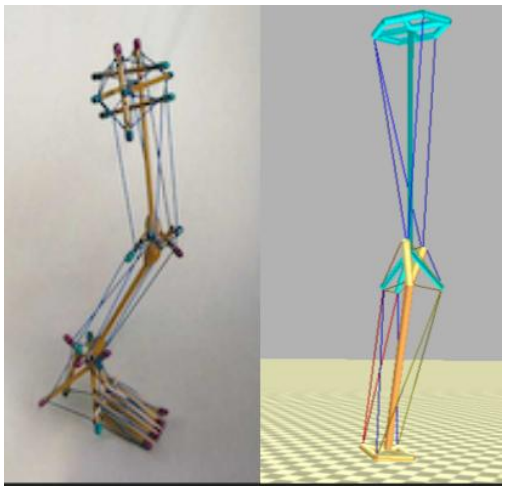

Figure 2.2: Final NTRT Model of Tom Flemons Knee Joint, [7]

placement, refer to model A in Figure 2.3. With the first few iterations of the models I used a baseline height of 10cm to allow easy manipulation and view of the entire model.

The second iterations, models B and C in Figure 2.3, included gravity and added more muscle groups to ensure that the model was stable. The main goal of these models were to ensure that the geometry was correct and that any extra muscle groups that weren't needed were omitted. From the first iteration it was seen that the models needed a rigid placement to the environment since the change in center of gravity may cause the model to fall over. When investigating how to constrain the model two options were presented, pin the model to the ground or to hang the model from a predetermined point. With the model pinned to the ground it was seen that flexion was achieved with the upper leg rotating towards the lower leg, but this caused an issue when determining the best tension elements to activate. From the current geometry the muscle group/ tension elements that would achieve maximum flexion would be the gastrocnemius or

calve muscles. When looking at the hung model the flexion was achieved with the lower leg rotating toward the upper leg. In addition to this the muscle group to cause max flexion was the bicepfemoral muscle group, which aligns with the anatomical correct muscles for flexion.

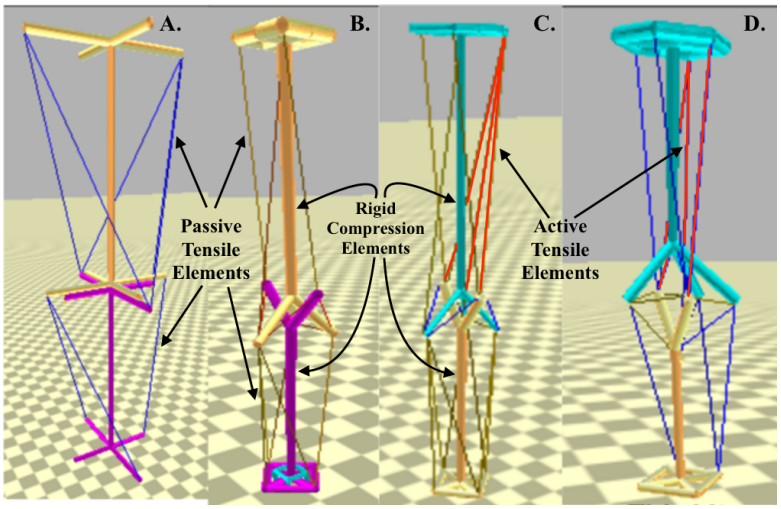

Figure 2.3: A: First Iteration, B: Second Iteration(Grounded), C: Second Iteration(Hung), D: Final Iteration

2.2.2 Controller

The controller that was used to determine how the structure would flex was made by activating specified muscle/tension elements. This controller type in NTRT is a tgBasicActuator, which is considered a perfect actuator. In the controller there is a time function and displacement function that monitors the active muscle/tension elements. When activating this muscle we set an initial muscle length and a desired muscle length. As the controller starts the muscle length is then adjusted until it either

hits the desire length or the model constraints cause the model to stop moving (cable interactions, solid element interaction, geometry failure, etc.). Depending on pretension and elasticity values of the tension elements the maximum change in muscle length could be adjusted. There are other more complex controller options such as kinematic motors where a motor is designed and torque is applied but since we are only looking at a simple motion that would need 1 to 2 motors at most a basic approach was determined.

In addition to the active actuation of the models there are passive forces such as pretension which applies a constant linear force along the tension element. This option was not changed for the second iteration of the model since it achieved the needed geometry but will be investigated for the final iteration. Lastly, an end effector and energy analysis script was included to determine the range of motion and energy needed to allow the model to perform flexion.

2.2.3 Final Iteration

The final iterations, model D in Figure 2.3, is just the Hunged model which has been modified by a factor of 5.08 to create a 4 foot model. This model contains material and environment conditions that would mimic a physical model made of dowel sticks. This approach closely mimicked the material list used in creating the human shoulder tensegrity structure [17].

For the NTRT simulations density, stiffness, and pretension were values that were adjust to reflect the physical model. From the bill of material in Table 3.4 the tension elements are the polypropylene elastic cord for the passive elements and high

strength Spectra cord for the active elements. In NTRT the pretension value relates to a the force in Newtons that is constantly applied. For this structure I used the ultimate tensile strength of a material to find the pretension value for the simulation. In regards to the 1/16" polypropylene elastic cord we have the following:

$$UTS_{(polypropylene)} = 28 - 36\ MPA\ or\ 10^6 N/m^2 [20]$$

$$Converting\ diameter\ of\ 1/16"\ to\ 0.15875\ cm$$

$$A = \pi * (d/2)^2 = 0.01979\ cm^2$$

$$UTS * A = UTS_{(Newtons)}, [(2800\ N/(cm^2) - (3600\ N/(cm^2))] * 0.01979\ cm^2$$

$$UTS_{(Newtons)} = 55.41 - 71.244N \rightarrow\ 60\ N\ in\ NTRT$$

In the regards to the Spectra fishing line it is rated for a max pound-force of 80 lbs. Using the conversion factor of $1\ N\ =\ 0.224809\ pound-force$ the max force of the line is 355.7 N.

For the density and stiffness values of the birch dowels I used the 0.00067 $kg/(cm^3)$ [21] and 5600N [22]. The stiffness NTRT is in kg/s^2 or N/cm so to get the max stiffness I used the longest element length of 50.8 cm to get 110.236 N/cm.

The geometry of the joint were also adjusted to fix an issue of cable interaction during flexion. This was adjusted in Model REV 1 and 2. The different geometries can be seen in the Appendix. The idea was to determine if the change in geometry would affect the workable range of the model and the amount of energy used during flexion.

2.3 Limitations and Consideration

By using NTRT there was a few limitation to the interacts that were in the models. From NTRT we can adjust all aspect of the environment and material properties, which uses the Bullet engine to generate. One of the limitations was cable interaction that may cause vibrations through the structure due to the geometry of the joint. In determining the muscle group attachment points and functions it was seen that if the muscles touched at any point in the simulation it would cause unwanted feedback. To mitigate against this the attachment points and pretensions were continually adjust so that vibrations were avoided or reduced.

Another limitation was the shapes at which the compression member could be made. The simulation only allowed straight compression members between the points. This didn't allow for curved members unless all points were mapped out along the curve. Lastly when trying to adjust pretension it was noticed that if the pretension was too high the tension element acted like a motor driving the model into that direction. This was seen to be an issue when trying to limit the max length a tension element can deform to help reduce compression members from touching.

2.4 Thesis Organization

The thesis is organized as follows: Chapter II presents the simulation and modeling of the tensegrity structure, Chapter III presents the build and design; Chapter IV presents the results and Chapter V presents the conclusions and future work.

Chapter 3

Physical Modeling

Using the simulated structure we adapted the coordinates of the model to make a 4ft model of the knee joint. Using coordinates from NTRT and uploading them into AutoCAD we were able to create models that could be used as building diagrams for the physical model. Below, Figure 3.1, depicts the entire structure as a whole and the major components.

3.1 AutoCAD and 3D Parts

The following are the AutoCAD drawings and models created with the factored coordinates from Table 3.1 and 3.2 and muscle attachment locations in Table 3.3. The point locations are displayed in Figure 3.2.

For the assembly of the dowel sticks to fit the overall geometry and attach to a base 3D printed parts were created. With the availability of a 3D printer it was determined for rapid prototyping that this was the best route to create a model. For

Knee Model REV 1 Points (cm) Scaling Factor[5.08]							
X	Y	Z	Point	X	Y	Z	Point
0	0	0	0	0	71.12	0	11
0	0	8.89	1	0	121.92	0	12
8.89	0	0	2	0	121.92	10.16	13
0	0	-8.89	3	5.08	121.92	0	20
-8.89	0	0	4	0	121.92	-10.16	16
0	50.8	0	5	5.08	121.92	10.16	14
7.62	60.96	0	6	-5.08	121.92	10.16	18
-7.62	60.96	0	7	5.08	121.92	-10.16	15
0	60.96	10.16	8	-5.08	121.92	-10.16	17
6.35	60.96	-6.35	9	-5.08	121.92	0	19
-6.35	60.96	-6.35	10				

Table 3.1: Knee Model 1 Point Table

Knee Model REV 2 Points (cm) Scaling Factor[5.08]							
X	Y	Z	Point	X	Y	Z	Point
0	0	0	0	0	71.12	0	11
0	0	8.89	1	0	121.92	0	12
8.89	0	0	2	0	121.92	10.16	13
0	0	-8.89	3	5.08	121.92	0	20
-8.89	0	0	4	0	121.92	-10.16	16
0	50.8	0	5	5.08	121.92	10.16	14
12.7	63.5	0	6	-5.08	121.92	10.16	18
-12.7	63.5	0	7	5.08	121.92	-10.16	15
0	58.42	12.7	8	-5.08	121.92	-10.16	17
10.998	58.42	-6.35	9	-5.08	121.92	0	19
-10.998	58.42	-6.35	10				

Table 3.2: Knee Model 2 Point Table

Knee Model Muscle Attachment Scheme		
Upper Body Muscles		
6-to-14	6-to-15	6-to-20
7-to-18	7-to-19	7-to-17
Upper Body Muscles		
5-to-8	5-to-9	5-to-10
6-to-8	6-to-9	7-to-8
11-to-6	11-to-7	10-to-7
Upper Body Muscles		
0-to-8	3-to-9	3-to-10

Table 3.3: Knee Model Muscle Attachment

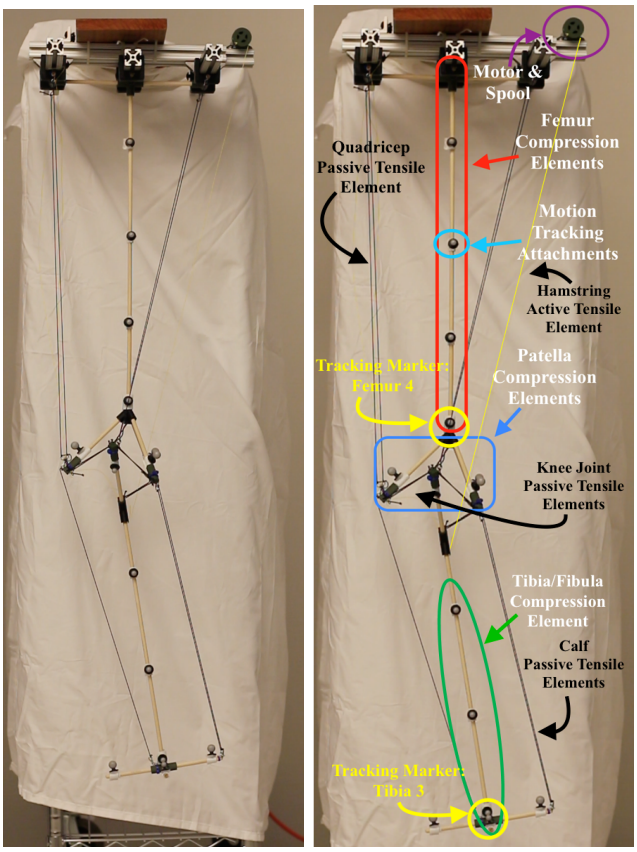

Figure 3.1: Proposed tensegrity knee joint, connecting femur and tibia equivalents. The joint is controlled by an active pair of strings tuned for stiffness creating a variable level of flexibility within the structure.

the Knee Model REV 1 CAD models a simple design was used to connect the dowel sticks. For the connection of the tension elements zip ties were used to attach the jack chain at the end of the dowel while a tension element with jack chains at the end hooks to these end points. The parts for points 0 and 12 are seen in Figure 3.3a, parts for points 14 and 16 are seen in Figure 3.3b, and finally parts 5 and 11 are seen in Figures 3.3c and 3.3d.

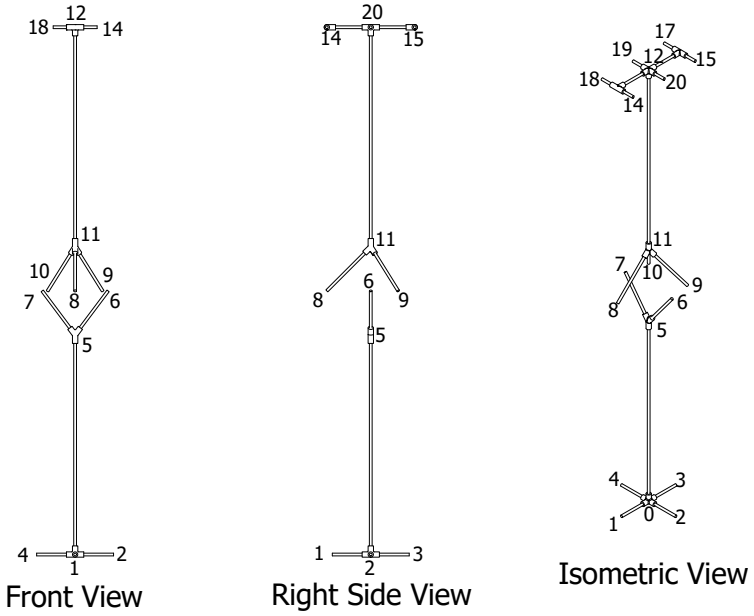

Figure 3.2: Knee Model Geometry with point definition

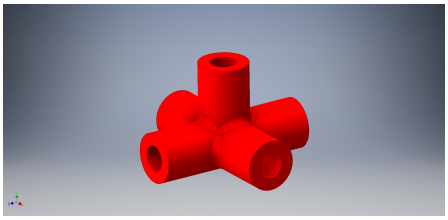

(a) Part for Points 0 and 12

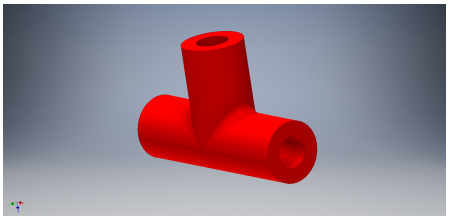

(b) Part for Points 14 and 16

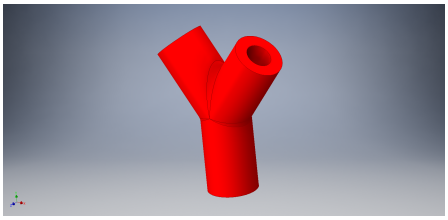

(c) Part for Point 5

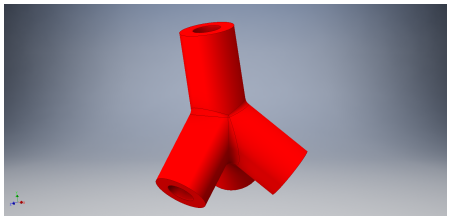

(d) Part for Point 11

Figure 3.3: Knee Model REV 1 CAD Parts

From the first iteration of the physical model, the attachment point became too congested, see Figure 3.4a. To mitigate these issues new end parts were printed for Knee Model REV 2 that contained holes to tread the elastic cord through and still keep it in the correct line of action and since we aren't using the jack chain anchors we can adjust the model faster for pretension. In addition to this, the geometry was changed to make the dimension as seen in the Appendix. Since this only affected the knee joint only points 5 and 11 were changed as seen in Figure 3.5. To ensure that the geometry would stay correct parts 6, 7, 8, 9, and 10 were made with holes to tread the elastic cord, refer to Figure 3.6.

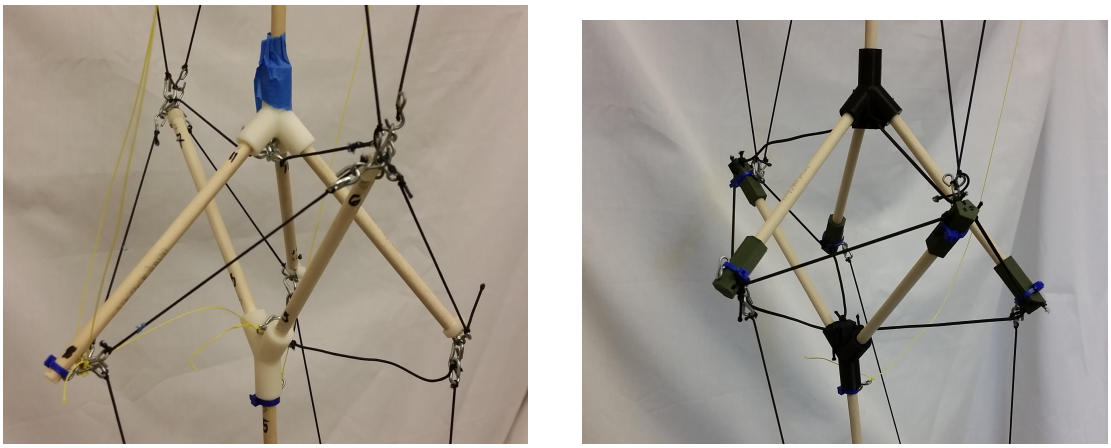

(a) Joint of Model REV 1

(b) Joint of Model REV 2

Figure 3.4: Joint Comparison from REV 1 to REV 2

In addition to these parts base attachments and motor spools were designed for these models. Using the specification from the motor listed in Table 3.4 the spools were designed to fit the motor shaft and allow for the Spectra cord force to be tangential to

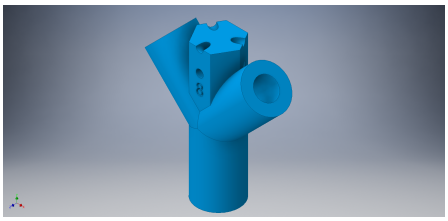

(a) Part for Point 5

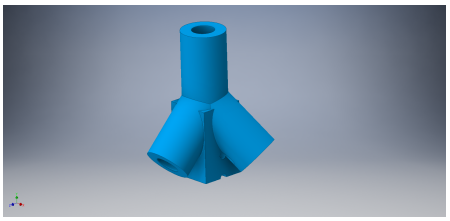

(b) Part for Point 11

Figure 3.5: Knee Model REV 2 CAD Parts

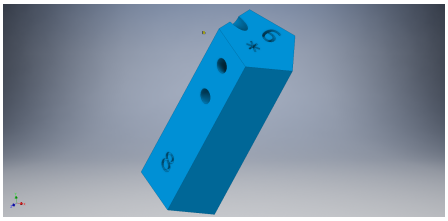

(a) Part for Point 6

(b) Part for Point 7

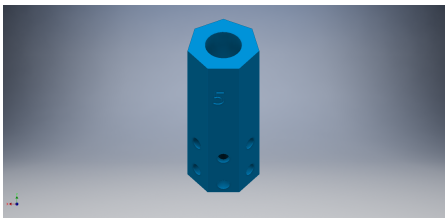

(c) Part for Point 8

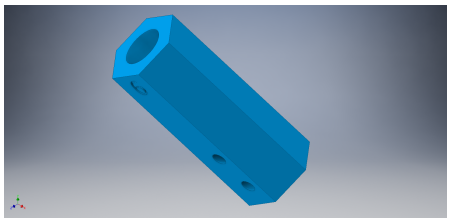

(d) Part for Point 9

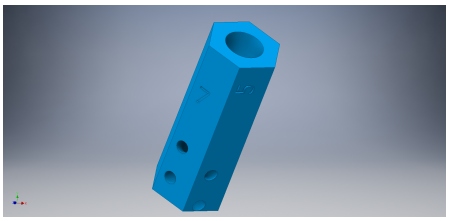

(e) Part for Point 10

Figure 3.6: Additional Knee Model REV 2 CAD Parts

the shaft. As for the base attachments they were designed to fit 1”x1” 80-20 T slotted aluminum framing using the 1/4-20 x .500” socket and T-nut hardware. The final design can be seen in Figure 3.8.

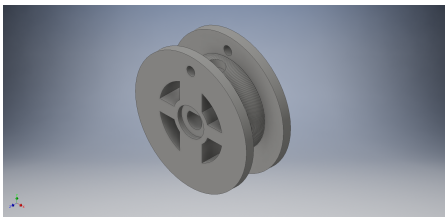

(a) Single Spool Part

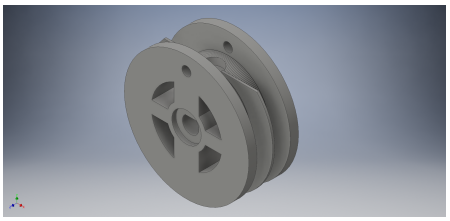

(b) Double Spool Part

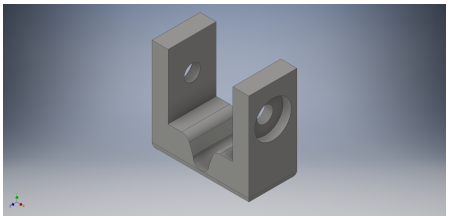

(c) Base Attachment Part

Figure 3.7: Addition CAD Parts

3.2 Hardware

The hardware used to build the physical models can be seen in Table 3.4, with the exception of the 80-20 Framing and fasteners as this was readily available in the lab. The framing used was the 1”x1”x1’ bars with the 1/4-20 x .500” socket and T-nut hardware. This aluminum framing can be viewed at https://8020.net/.

The Ardunio micro-controller and motor shield, see Figure 3.9, were used due to ease of use and ability to handle up to four DC motors. This was following the

Bill of Materials			
Item	Price	Quantity	Total
154:1 Metal Gearmotor 20Dx44L mm	19.95	4	79.80
Pololu 20D mm Metal Gearmotor Bracket Pair	6.95	2	13.90
Zinc-Plated Jack Chain	5.00	1	5.00
Dritz 9342B Round Cord Elastic, 1/16-Inch	5.00	3	15.00
Power Pro Spectra - 150 yd. Spool - 80 lb. - Yellow	20.00	1	20.00
1/4in Wooden Dowel	0.55	4	2.20
Arduino Uno R3 (Atmega328 - assembled)	25.00	3	75.00
Shield stacking headers for Arduino (R3 Compatible)	1.95	4	7.80
SunFounder DC 9V/650mA Power Plug Adapter for Arduino UNO R3 Mega 2560 1280	5.99	2	11.98

Table 3.4: Bill of Materials

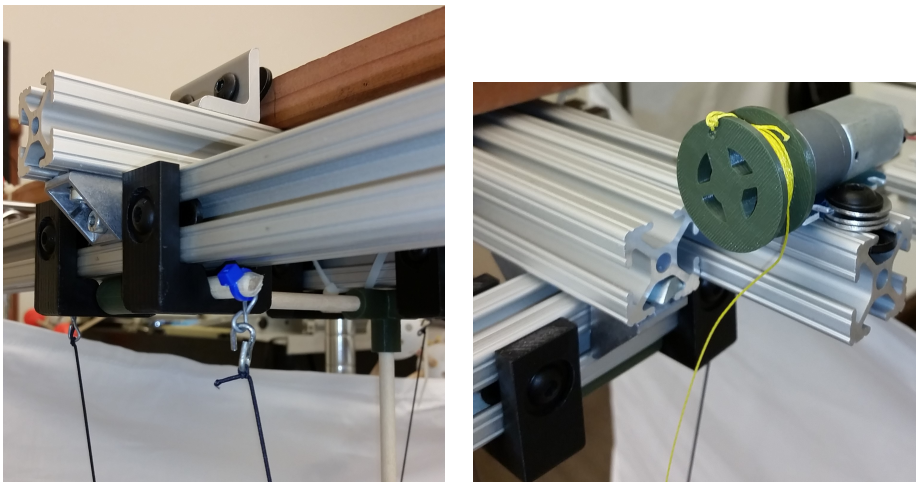

(a) Base Attachment (b) Motor and Spool on Base

Figure 3.8: Base Parts on Physical Model

setup of the physical models from [15]. The code used in the Arduino is a simple while loop that initiates the code and runs it once the unit is powered up. To help control when we want the motor to turn on a simple button circuit was setup to send an "ON" signal to Pin 2 of the Arduino I/O pins when decompressed. The circuit of this 4 prong switch/button is seen in Figure 3.10.

For the actuation of the physical model simple torque analysis was done on a completed frame. The total weight of the model was 73.6 grams and rounded to 75 grams for a better estimate. The total length of the model was 116 cm which each which the upper and lower segments both around 58cm in height. To find the max torque needed to lift the entire model the total weight and length were used in the following equations:

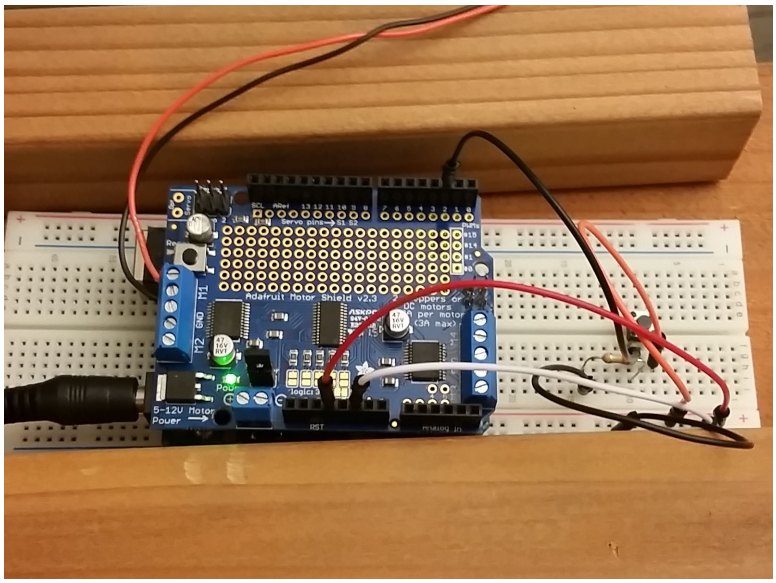

Figure 3.9: Arduino with button circuit

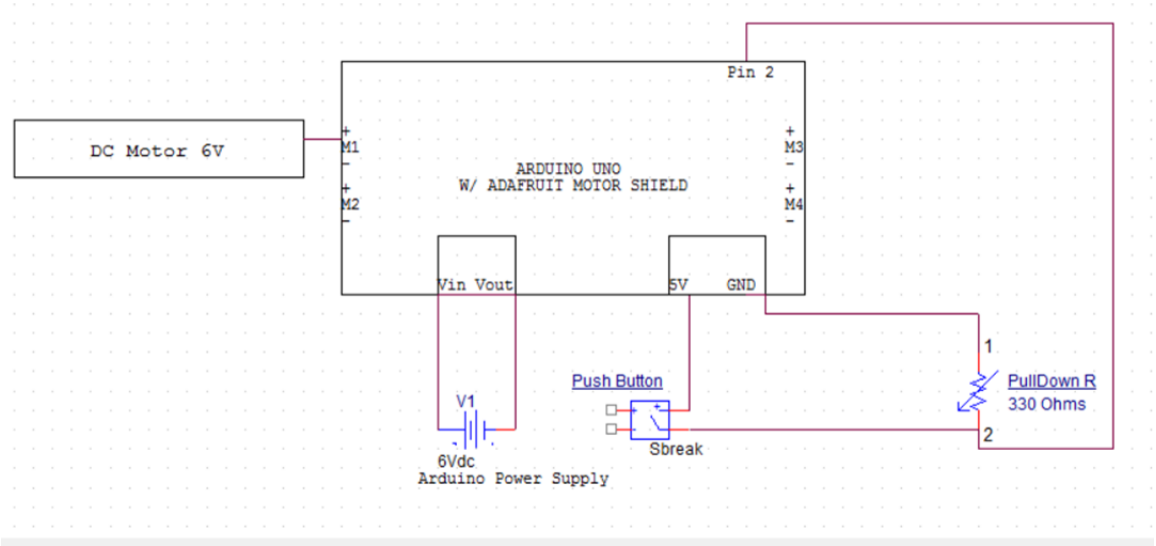

Figure 3.10: Circuit for Arduino, Motor, and Push Button

$$Force \ = \ mass \ x \ acceleration \ (gravity)$$

$$Force \ = \ 75 \ grams \ x \ 981 \ cm/s^2 \ = \ 0.73575 \ Newtons$$

$$\tau(torque) \ = \ Force \ x \ Length$$

For torque two equations were used: 1) The actual max torque, which is when the length is actually 58 cm and the total mass is at the end of the length, 2) The max torque, which has the length at max length and total mass is at the end of the length.

$$\tau_1 \ = \ 0.73575 \ N \ x \ 58 \ = \ 60 \ oz - in$$

$$\tau_2 \ = \ 0.73575 \ N \ x \ 116 \ = \ 120 \ oz - in$$

The overall goal for the motor was to find a DC motor that could produce a torque of 60-120 oz-in, run at 5 Volt (highest voltage supplied by Arduino that is independent of power source), light-weight, and max at 3 Amps (max current that the Motor Shield could deal with). In light of this the best motor for the project was the Pololu 154:1 Gearmotor, Figure 3.11 and 3.12, with a max torque of 120 oz-in, voltage at 6 V, a weight of 44 grams, and 3.2 A at stall. Since the max torque (τ_2) was considered the worst case scenario the stall current of 3.2 This was deemed safe for the motor shield as long as only one motor was used at a time. As for the voltage needed a work around was done to have the supply voltage to the Arduino at 6V and the jumper pin for the Motor Shield was set to use the supply voltage.

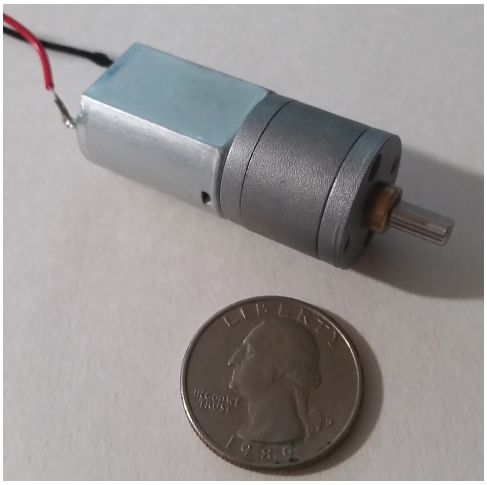

Figure 3.11: Pololu 154:1 Gearmotor

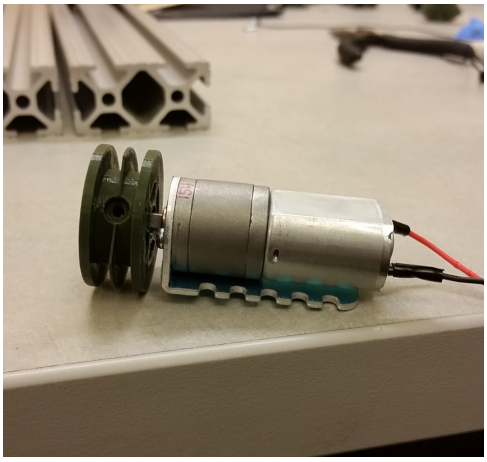

Figure 3.12: 6V DC Motor with Spool

Chapter 4

Results and Comparison

The experiments were performed in the engineering building at the University of California, Santa Cruz.

4.1 Simulations

The following ,Figure 4.1, depicts the motions of the Matlab and NTRT models. From these Figures it can be seen that the range of motion that we wanted to achieve was not met in both models. For the Matlab model the max angle was 90 degrees while the NTRT models were about 120 degrees. For the Matlab model the motion was achieved by tracing the Y coordinate from 0 to 30 cm, which was the achievable work space. For the NTRT model the geometry was the limiting factor with the forces of the joint causing errors if the lower leg was pulled too far.

In Figure 4.2 we tracked the X-Y-Z coordinate displacement of the end effector on the base of the leg in the last two model revisions (REV 1 and REV 2). The NTRT

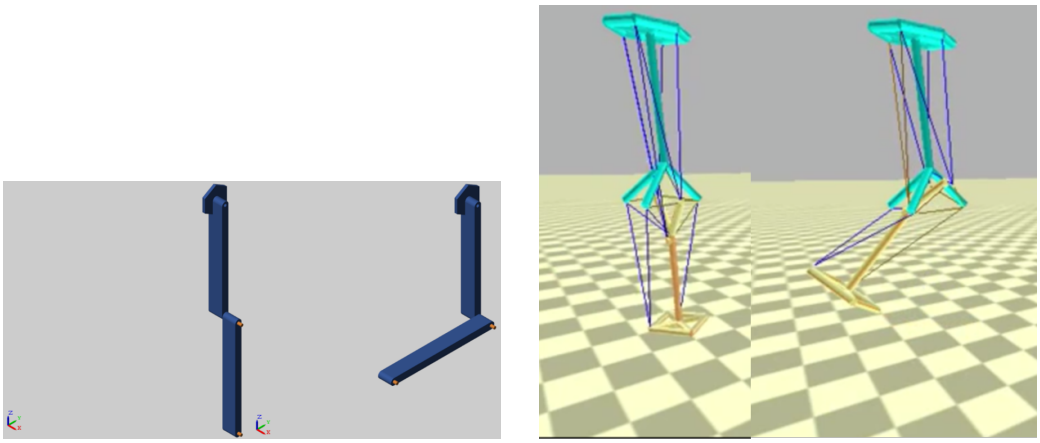

(a) Matlab Motion(Need to Update with Physical Dimensions)

(b) NTRT Motion(Need to Update with Physical Dimensions)

Figure 4.1: Depiction of Motion

simulations were plotted into Matlab to get a visual representation of the movements. For the Matlab knee model it could be seen that the displacement was on along the Y and Z plane, which makes sense since the force and and movement is restricted to a linear plane. Referring to Figure 4.2a, there are significant differences between the range and steadiness of motion. The plots show convincing evidence that the degree positioning of where the compression elements are angled provide the tensegrity structure with a wider range of motion. The other significant results is the difference in stability between structures. The motion of the system shows REV 2 with smooth parabolic displacement during the flexion of actuated muscles, while the REV 1 lacked that particular feature in its results. Each tensegrity structure performs its task of flexion through the simulated actuation of cables to act as muscles. In essence the Matlab model can only reach up and down, while the NTRT model is able to have multiple paths depending on force

applied.

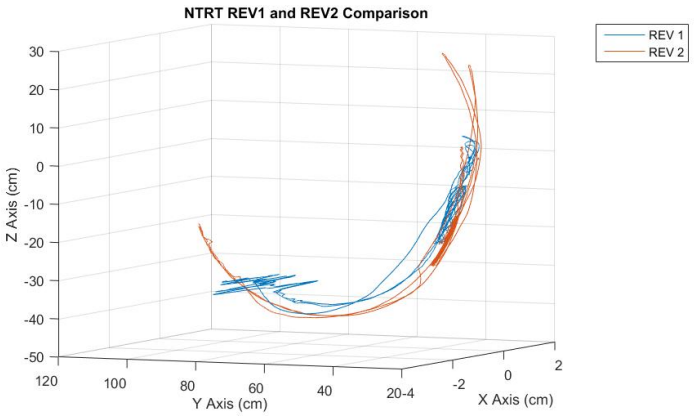

(a) Model REV 1 and REV 2 Position Data

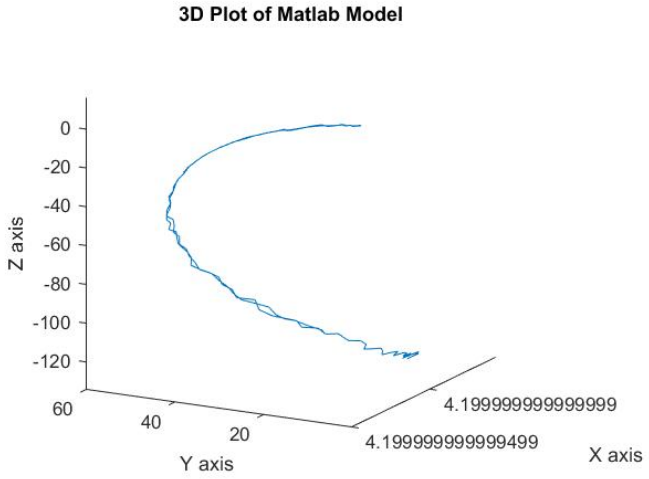

(b) Matlab Hinge Model Position Data

Figure 4.2: Position Data

For the amount of force needed for actuation the simulations were investigated to determine an approximate force. In Matlab the rotational force needed can be seen

in Figure 4.3. This data was gathered by the Matlab Simulink Revolute Joint module and only reflects the rotational force needed to overcome gravity. This was due to the complexity of the NTRT software. From the Matlab data it was seen that the max torque needed for actuation of the lower leg was about 0.12 N$*$cm. For the NTRT scripts we attempted to use the built-in getTension() function for the active muscle, which used the equation $Tension = stiffness\ x\ (currentLength - restLength)$, but this approach used a high stiffness value that didn't correspond to the elastic cord. To get an approximate of the tensile force/stress in the cord the relation between Young's Modulus, 0.01 GPa for elastic type cord including rubbers [20], and change of length was used. For this equation $dl = change\ of\ lenght$, $\sigma = stress\ /\ tensile\ force$, $I_o = initial\ length$, $E = Young's\ Modulus$, and $A = cord\ cross-sectional\ area$.

$$Tensile\ Force(Newtons) = (\sigma * A) = (A * ((\ E * dl\ )/I_o))$$

From this equation we have the following graphs for tensile force for models REV 1 and REV 2, Figure 4.4. In these plots the max force needed is between 6.9-7.5 Newtons, which correlates to the range that the physical models can achieve. It is important to note this is an approximate to the tensile force needed. This method doesn't include resistive forces due to gravity and other tension elements. From the simulation the change in length is the actual change of length as the basic actuators "spool" the elastic cord, as the program doesn't track the elastic deformation of the elastic cord. This in-turn makes this value a very conservative approximation for tensile force.

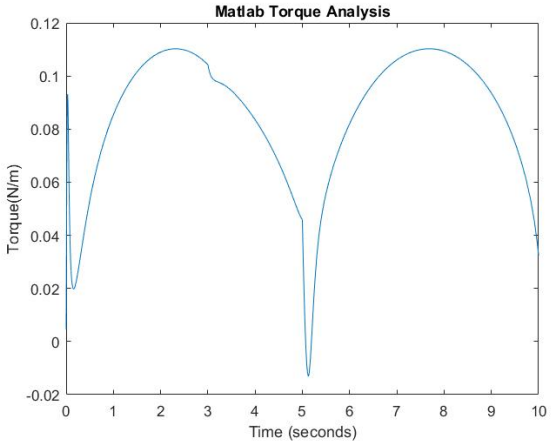

Figure 4.3: Torque data from Matlab model

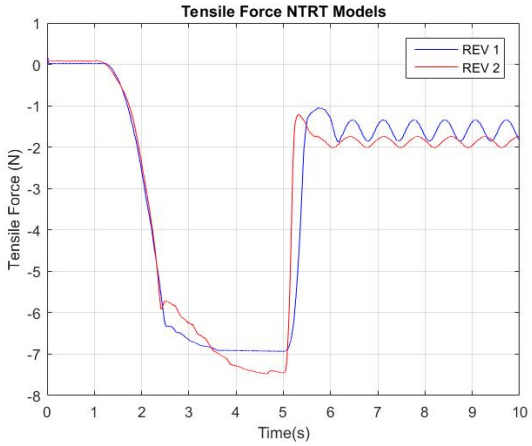

Figure 4.4: Tensile Force data for NTRT models

4.2 Physical Model

While constructing and actuating the physical models it came to our attention that the upper leg segment started to bend in a way that caused concern. In addition to this we noticed that compression elements were touching at max flexion. Figure 4.5 depicts the bend and Figure 4.6 depicts how the compression elements would touch for

both REV 1 and 2 first iteration.

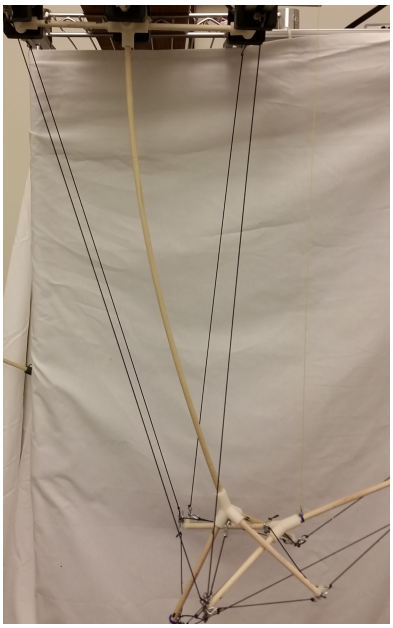

Figure 4.5: Bending Compression Element

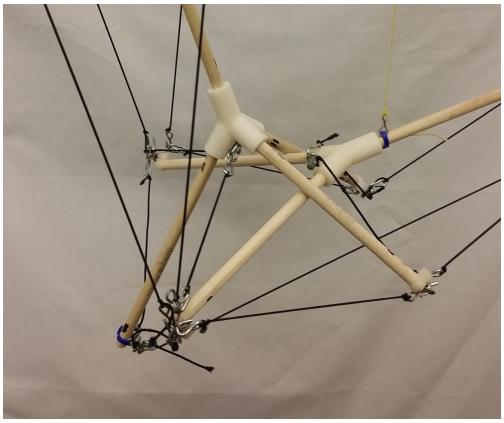

(a) REV1_1 Touching

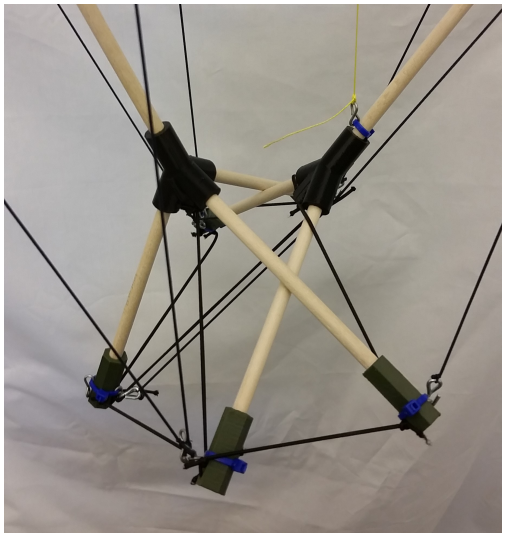

(b) REV2_1 Touching

Figure 4.6: Compression Elements Touching in first iteration of REV 1 and 2

To mitigate both of these issues we created second iterations of both models and called them REV 1_2 and REV 2_2. In these models we replaced the tension element from Points 5 $\rightarrow$ 8 with the Spectra cord. This would allow so less elastic deformation which in turn would reduce the touching of the compression elements. Spectra cord was also added to Points 14 $\rightarrow$ 8 and 18 $\rightarrow$ 8 to apply a resistive force against the moment/torque that was being applied by the force of flexion. In Figure 4.7 we see that there is a difference in position from both models. With REV 1_2 we see that the geometry still constrains the motion of flexion and at the peak the compression elements still touch. With REV 2_2 the geometry helps achieve max flexion without letting the compression elements touch.

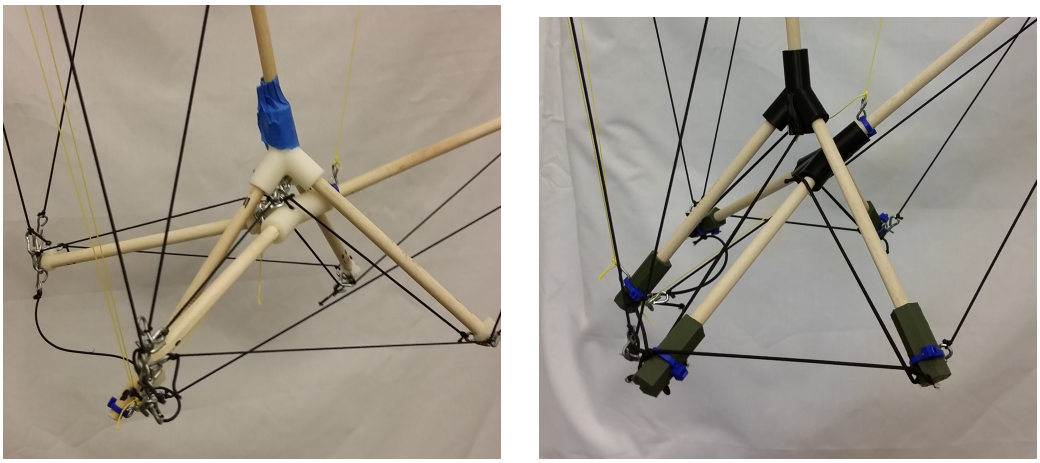

(a) REV1_2 Touching

(b) REV2_2 Touching

Figure 4.7: Compression Elements Touching in second iteration of REV 1 and 2

To better analyze the motion of the physical model we used a video tracking software KINOVEA. In this program we can set up a pixel tracker that monitors and

KINOVEA Angle Data		
Model	Bend Angle	Flexion Angle
REV 1_1	13°	106°
REV1 _2	10°	99°
REV 2_1	11°	109°
REV 2_2	4°	118°

Table 4.1: KINOVEA Data

sketches the trajectory of an object. For the physical models we tracked the "bend" of the upper leg segment that occurred when the flexion was at its peak, and the angle of flexion relative to initial position of Point 11 of the upper leg segment.

The following Figures are the visual results from the KINOVEA software. For all of the Knee Model REV 1 analysis we looked at the timestamps of 0, 2, 5, and 7 seconds. For all of the Knee Model REV 2 analysis we looked at timestamps of 0, 3, 6, and 9 seconds. These timestamps are located on the bottom left of each image. This data is also compiled in Table 4.1.

From this data we see that overall the inclusion of the Spectra cord for the second iterations of the models was able to reduce the "bend" in the upper leg segment. In addition to this the geometry difference between Model REV 1 and 2 seems to have impacted the allowable flexion angle, with Model REV 2_2 having the closes flexion angle that reflects the actually human knee (160°). For purposes of this project and the application for next generation rehabilitation and prosthetics the angle of 120° would

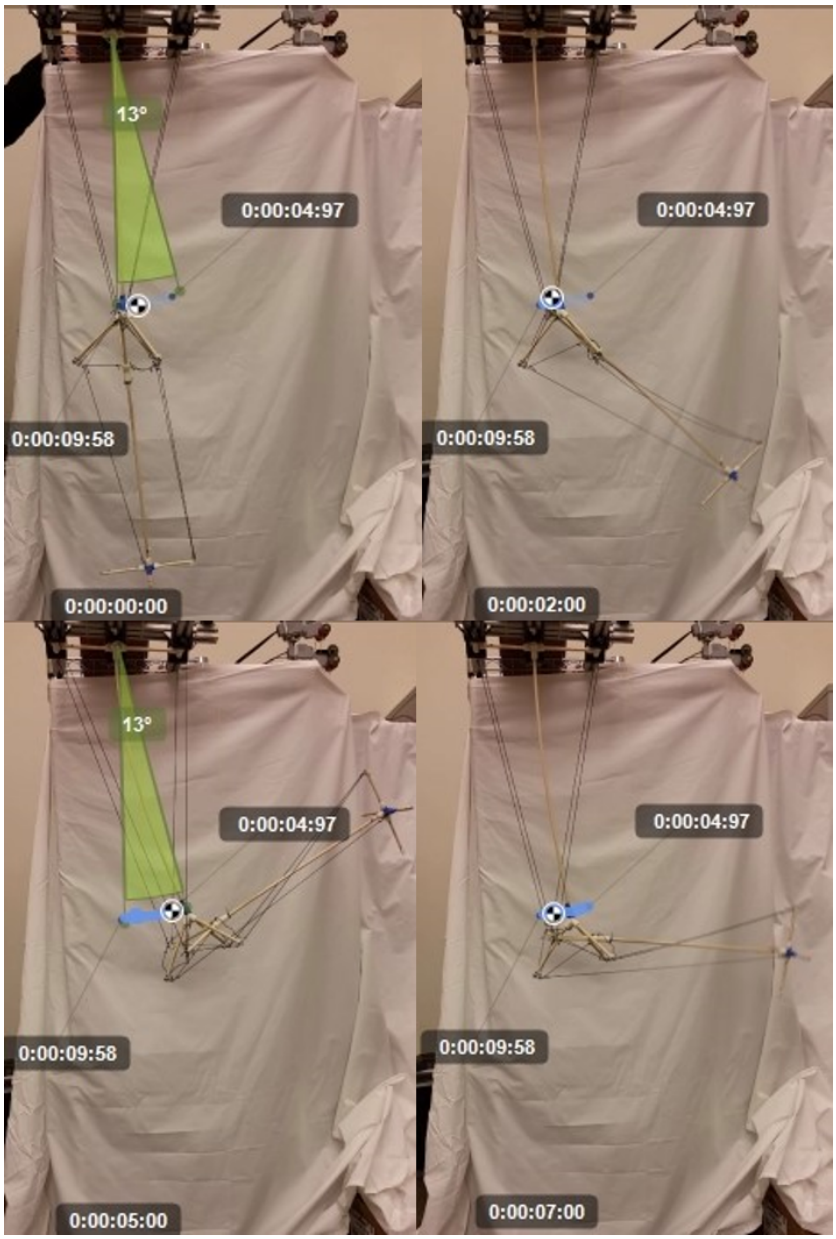

Figure 4.8: REV1_1 Bending

be an achievable goal as existing knee prostheses do not allow a full return to normal activities for this large population since they are limited to achieving knee flexion of about 120 degrees [24]. These data points are approximates as the KINOVEA software

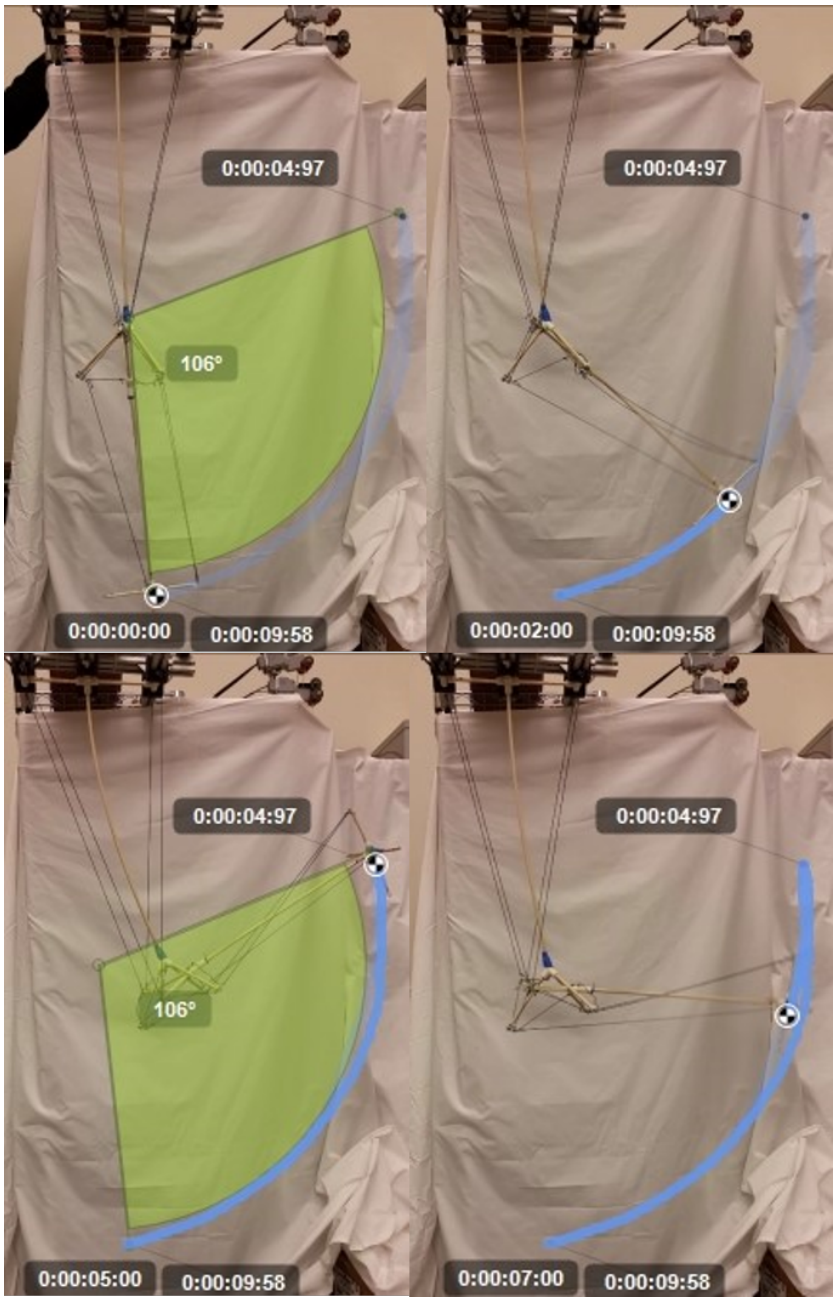

Figure 4.9: REV1_1 Flexion

had jumps and would lose the tracking pixel if the point moved across one of the dark colored tension elements. For a more accurate representation for the movements of the

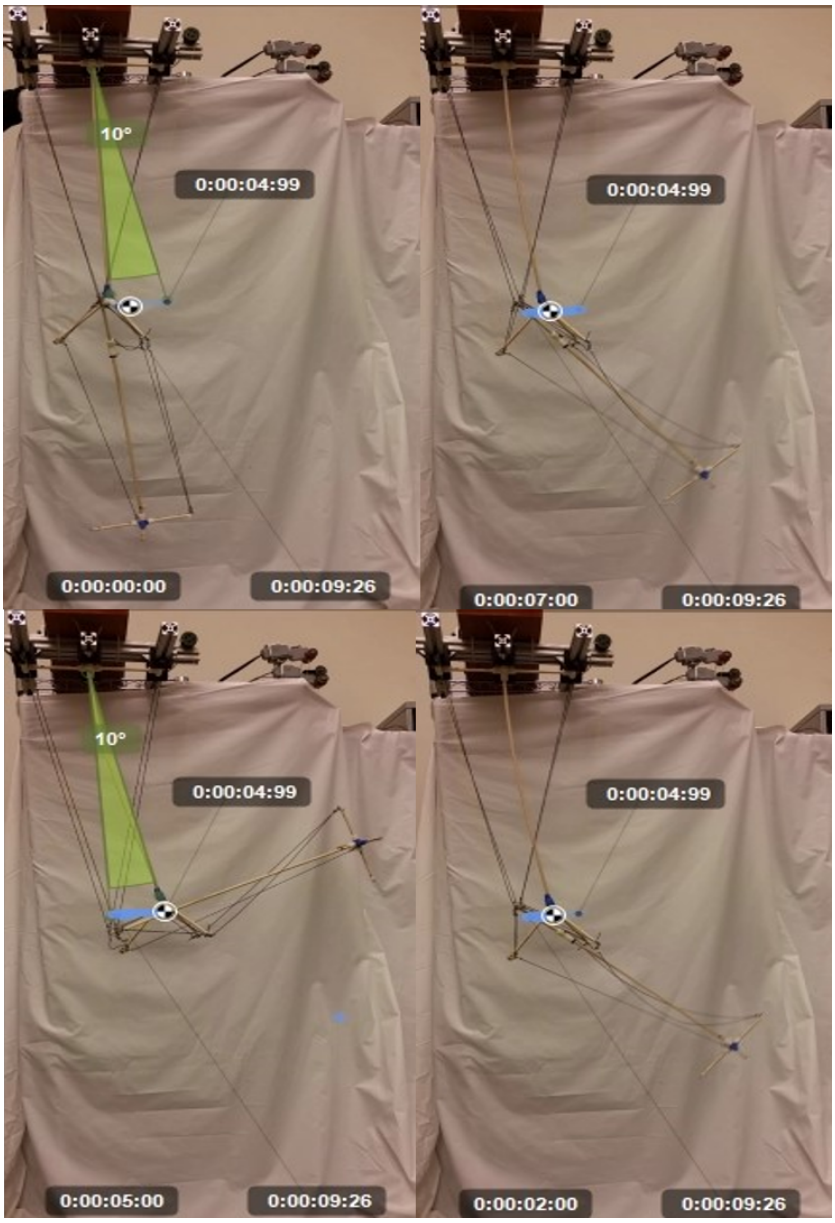

Figure 4.10: REV1_2 Bending

physical model the OptiTrack system was used. OptiTrack allowed us to track reflective balls that we attached to the Tensegrity leg and to see their positions with more accuracy as the leg moves. We were also able to gather the coordinates for every reflective trackers

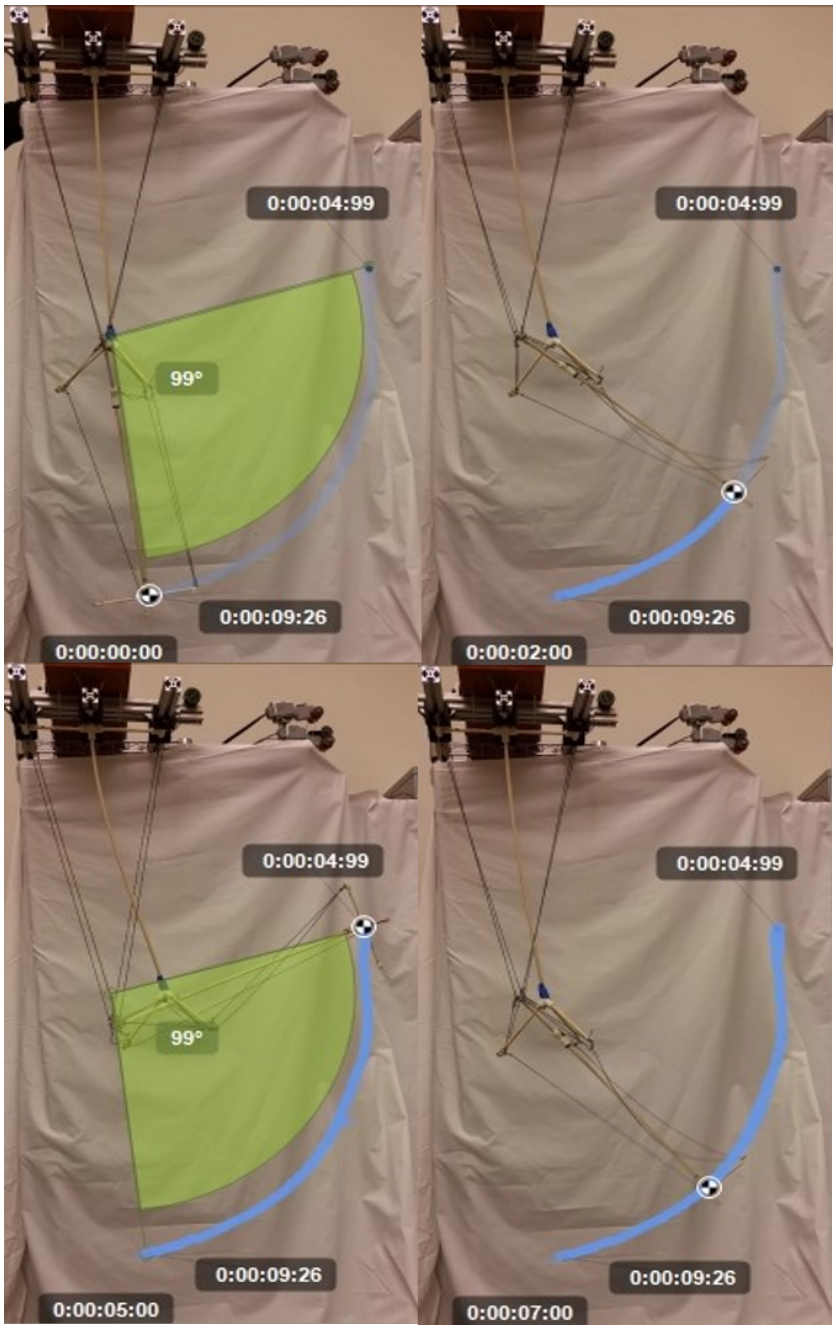

Figure 4.11: REV1_2 Flexion

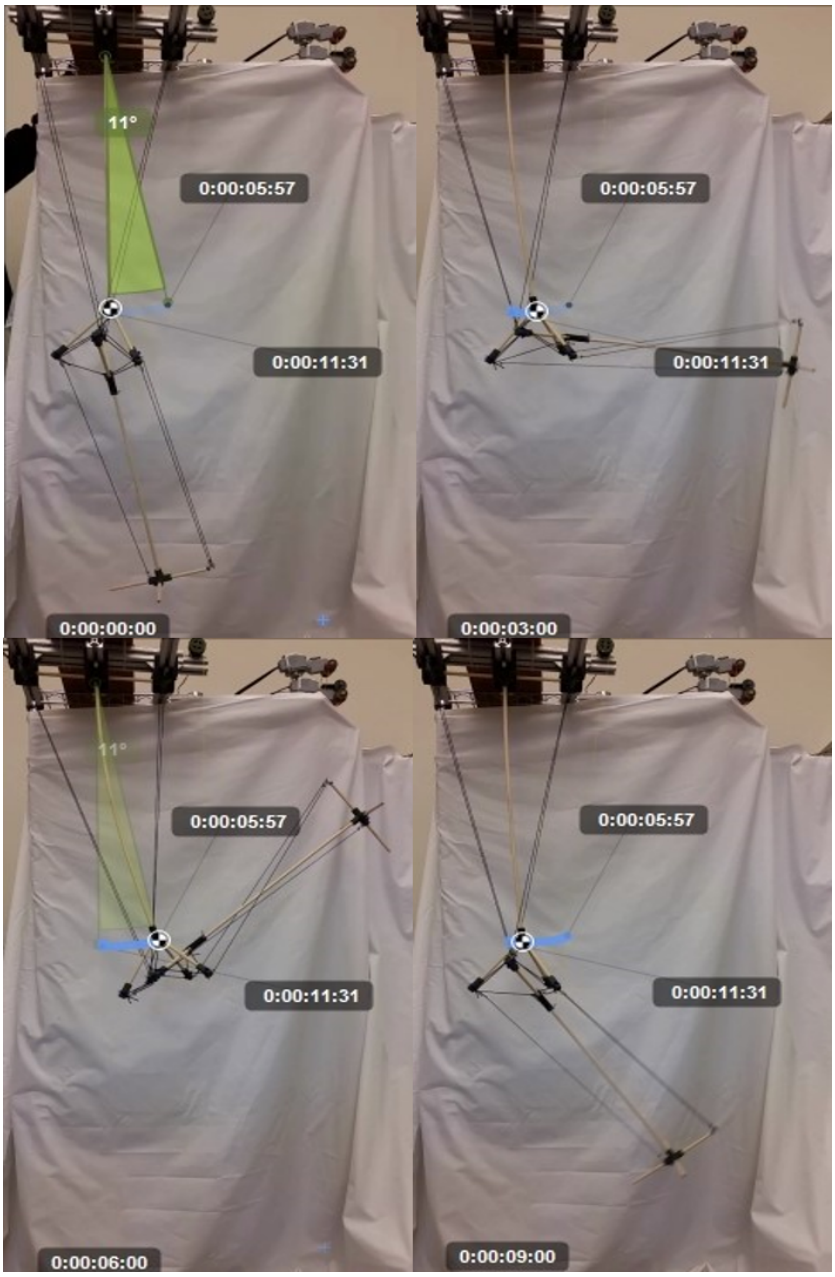

Figure 4.12: REV2_1 Bending

as the knee joint flexed which is more than the single point that KINOVEA is able to track. For the OptiTrack we only measured the REV 1_2 and REV 2_2, as these two

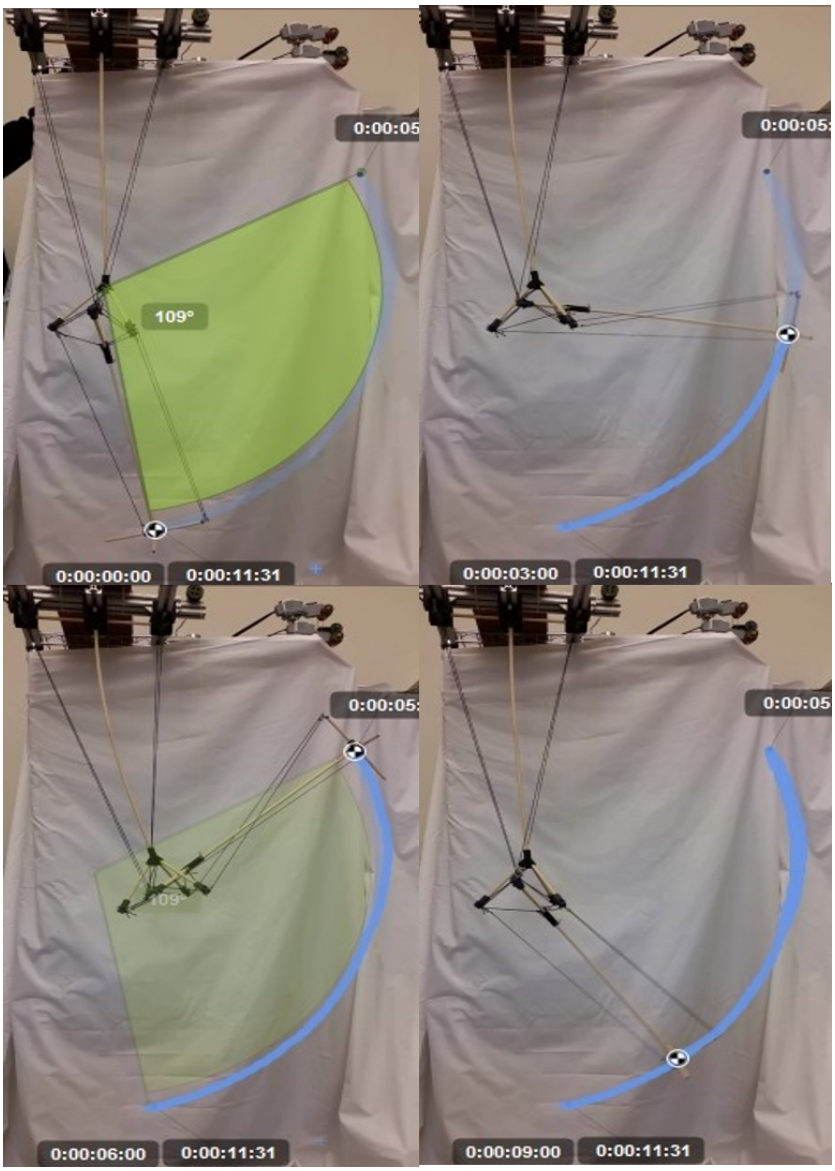

Figure 4.13: REV2_1 Flexion

models more closely aligned to the motions of the simulation, which was without the bend in the femur element.

With this data, we also calculated the actual angle from start to finish of our first and second physical prototype. Our first design (REV 1) was only able to achieve

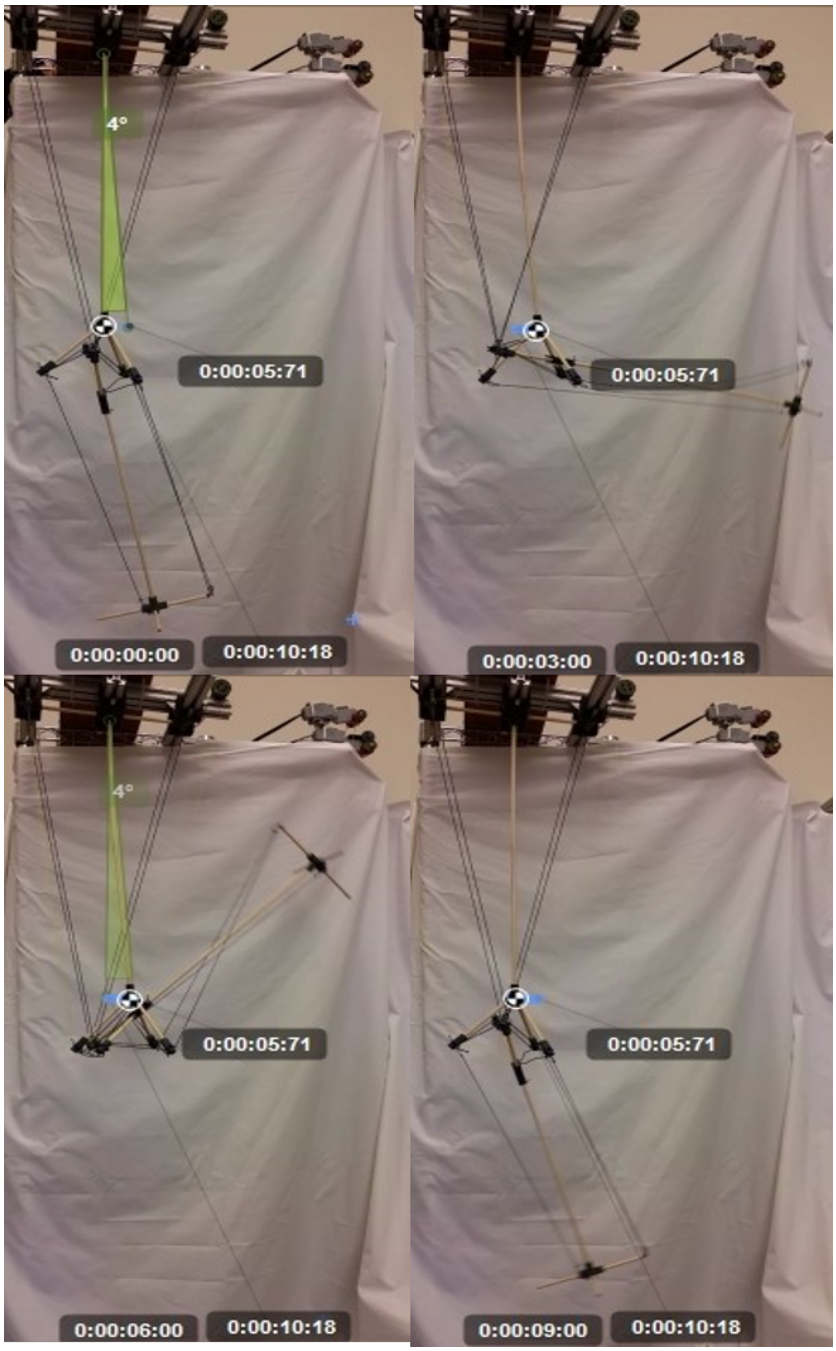

Figure 4.14: REV2_2 Bending

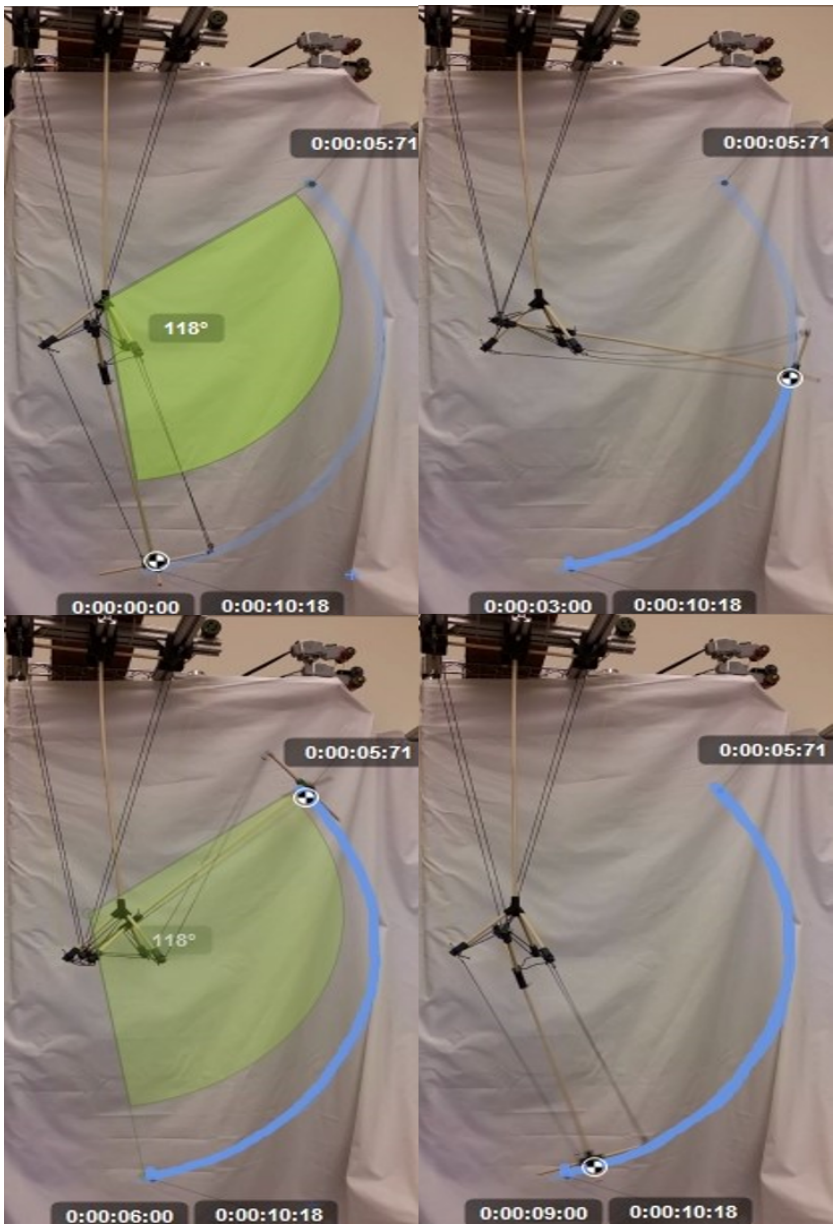

Figure 4.15: REV2_2 Flexion

a maximum angle of flexion at 91 degrees, whereas with the new design (REV 2) we could achieve an angle of 129 degrees, which correlates to the 120 degrees that existing knee prostheses achieve [24]. Referring to 4.18, REV 2 reaches a higher point in the

y-axis while the femur maintains a position closer to equilibrium. REV 1 happens to not maintain the initial equilibrium on the femur and stresses the compression elements. This specific tensegrity leg was created to maintain its structural stability while being able to flex and put stress on the passive tensile elements on the structure. The passive tension components allow the structure to absorb external forces and distribute it evenly across the knee joint. This allows the structure to keep flexing without the worry of breaking the compression element similar to Figure 4.19.

The process towards calculating the angle displacement shown in Figure 4.19 and 4.20, was by using the *Tracking Marker: Femur 4* in Figure 3.1 as a point of origin. In both mechanical revisions, for the tensegrity structure, we used the same location for the markers and calculated the angle based off of the displacement from the *Tracking Marker: Tibia 3* in Figure 3.1.

$$\cos(\alpha) = \frac{\bar{x} \cdot \bar{y}}{|\bar{x}| \cdot |\bar{y}|} \tag{4.1}$$

Using the distinct anchor points, for the tensegrity structure *Tracking Marker: Femur 4* we found the angle of displacement for both REV 1 and REV 2. For the physical models, REV 1 and REV 2, we also tracked the "bend" of the upper leg segment that occurred when the flexion was at its peak, and the angle of flexion relative to initial position of the upper leg segment. When referring to Figure 4.21 and 4.20, we are able to see a significant difference between the equilibrium and flexed position.

Table 4.2: Positions of Leg From OptiTrack

Model Version	Tracking Marker	X (m)	Y (m)	Z(m)
REV 1	Femur 4	1.5183	0.9321	1.1522
REV 2	Femur 4	1.5667	0.9206	1.1620
REV 1	Tibia 3 at t_0	1.6996	0.4195	1.1579
REV 1	Tibia 3 at t_{33}	1.9234	1.0270	1.160
REV 2	Tibia 3 at t_0	1.5893	0.3988	1.1559
REV 2	Tibia 3 at t_{26}	2.0506	1.4986	1.1416

Table 4.3: Parameters of Leg Vectors

Model Version	Vector	X (m)	Y (m)
REV 1	x	0.1328	-0.5011
REV 1	y	0.3566	0.1064
REV 2	x	0.0710	-0.5333
REV 2	y	0.5322	0.5665

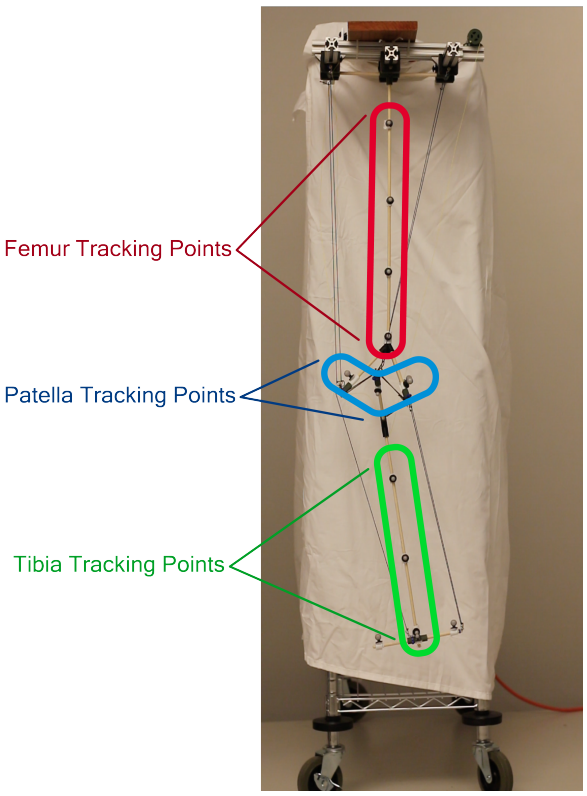

Figure 4.16: The OptiTrack system uses motion capture markers for precise localization. The femur tracking points were marked in the system 1 through 4 from top to bottom. The arrangement for patella is marked from left to right for 1 through 3. Lastly, the tibia tracking points are marked similar to the femur, top to bottom 1 through 3.

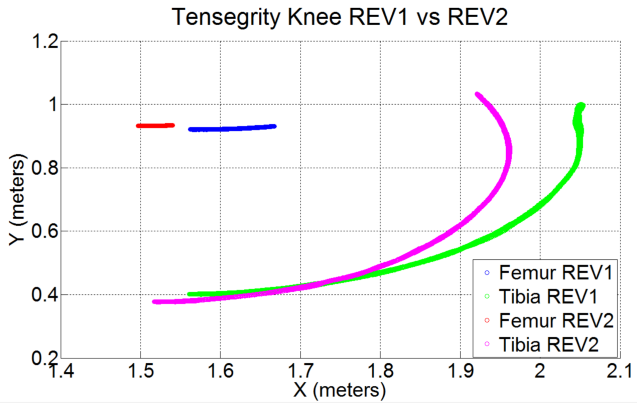

Figure 4.17: In this figure, we tracked the displacement of the knee as it flexes. As shown in Figure 4.16, we used the tracking markers, Femur 4 and Tibia 3. Femur 4, shown in blue (REV 1) and red (REV 2) are used as the reference point as Tibia 3 flexes. We can see that the femur (red) doesn't move as much as the blue (REV 1) one, which tells us that our revised structure is more stable. We can also see that in REV 2, the tibia 3 tracker (magenta) is able to achieve a larger range of motion than the tibia (green REV 1) and stays on its motion path throughout the whole flexion of the tensegrity knee.

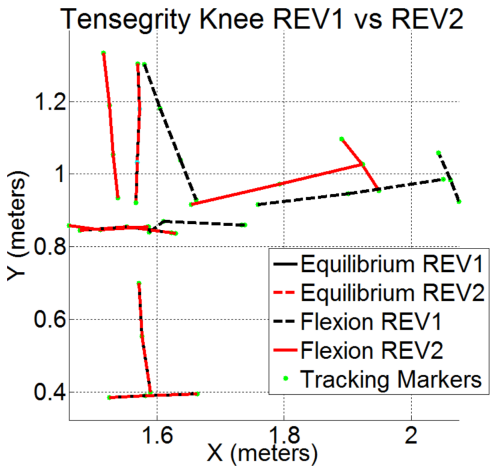

Figure 4.18: Using the OptiTrack motion system, we aligned the initial position of both REV 1 and REV 2 of the tensegrity leg. This flexion period of both models, REV 1 (in black) and REV 2 (in red), show a significant difference in the final position.

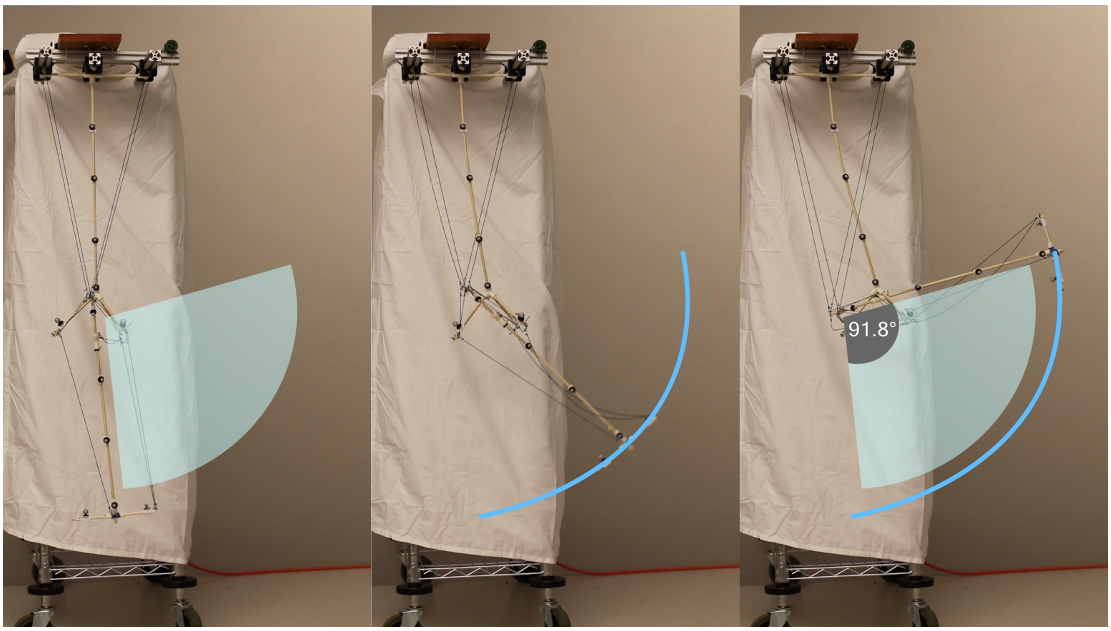

Figure 4.19: Tensegrity knee REV 1 Flexion. This model can only flex 91 degrees.

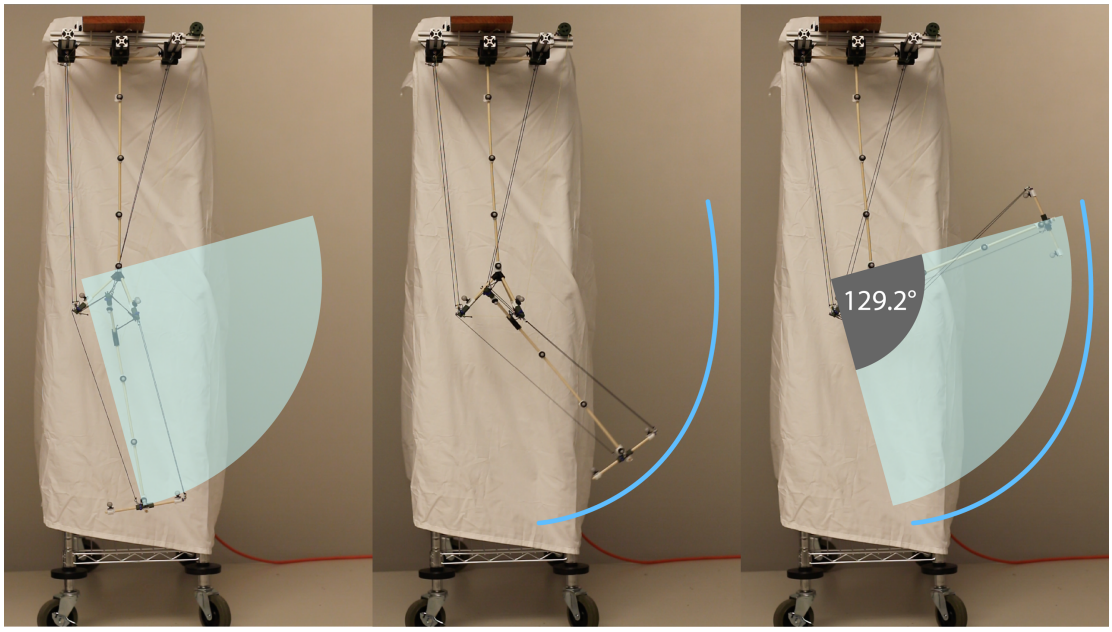

Figure 4.20: Tensegrity Knee REV 2 Flexion. Unlike figure 4.19, this model is able to flex 129 degrees.

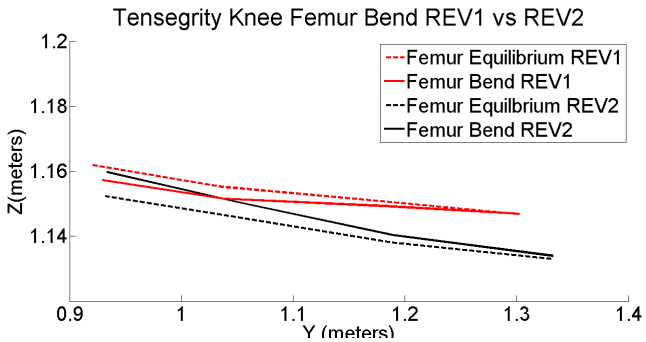

Figure 4.21: This figure represents the amount of displacement within the femur just from the flexion of the structure. The REV 2 design handles the stress of the system by properly placing antagonistic tensile elements to provide a counter force. These additional tension elements reduces the stress on the femur components showing a significant difference from equilibrium to bent.

Chapter 5

Conclusions and Future Work

In conclusion we were able to attain a good understanding on how the Tensegrity joint compares to classical hinge joints when modeling the human knee. From the data it was seen that the hinge joint only has a limited range of motion where as the tensegrity structure can operate in two different axis, if controlled properly. From the tensile force and torque analysis in Matlab and NTRT it was found that the Matlab model of a simple hinge design, equivalent to the NTRT model, required less force for actuation. This is only for actuation and doesn't look at the capabilities when a load is applied to the system.

From the different geometries used in our simulated and physical models we saw the effects it can have on the range of motion and stability of the models. In addition to this the combination of elastic cord and Spectra cord to stabilize the models brings to light the needed complexity to create the knee, as this type of material deflection and string control was not simulated or achievable in NTRT. In the next iteration of the knee,

active joint muscles will be needed to finely control both the flexion and extension of the knee. This will be helpful when creating a self standing or walking tensegrity structure. The final result was the ability to successfully simulate a tensegrity representation of the knee in NTRT and create physical models to verify the simulations movements. Even though this is a simplified version of the complex knee joint, more work is needed to create a more complex and efficient representation of the knee.

Future improvements to this model would be a rearrangement of attachment points to accompany the knee extension, which was out of scope for this project. As with the tensegrity arm and shoulder models [15] the effect of complex motions and external force effects on the motion and capabilities of the system needs to be investigated. This would come into play when other motions are introduced to the knee model and if a hip or ankle joint is attached.

Chapter 6

Appendix

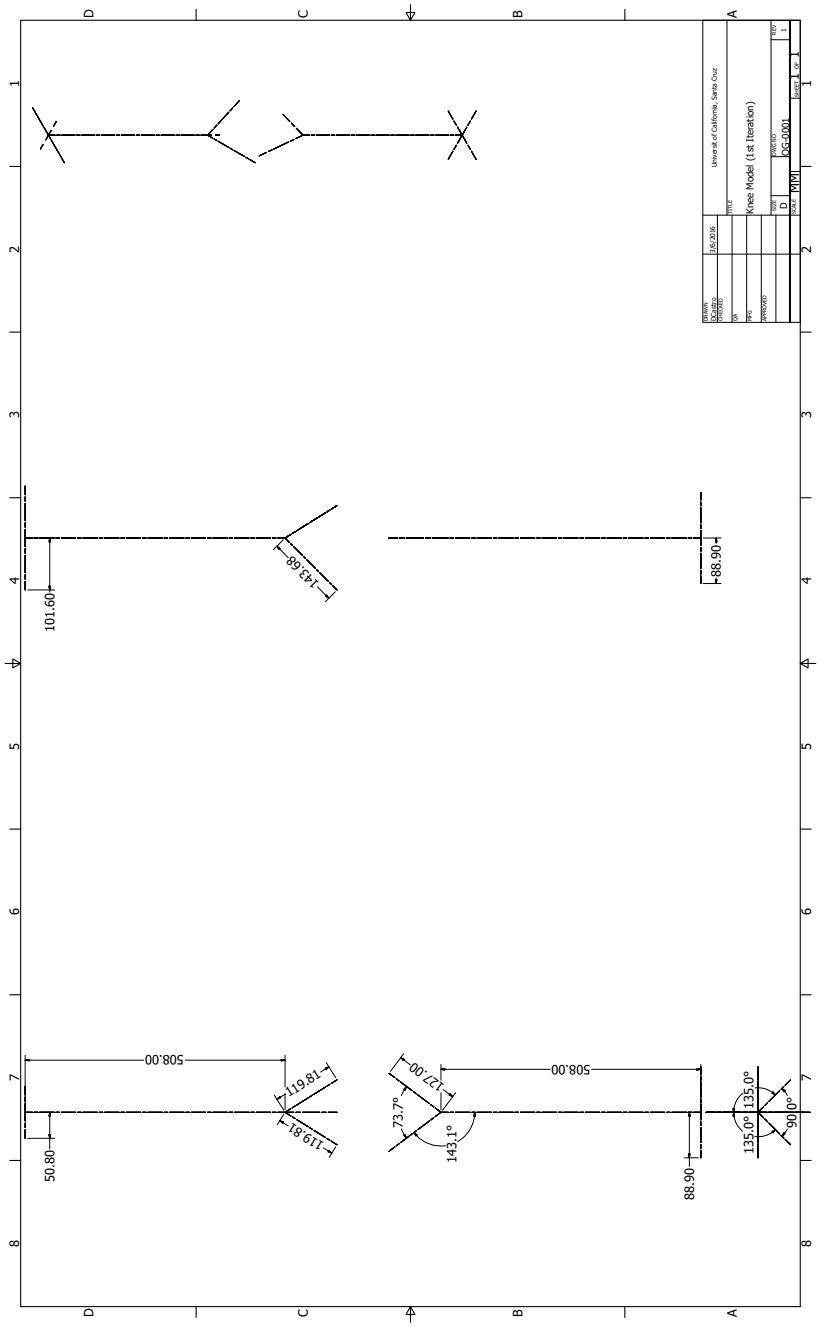
D
C
B
A
1
2
3
4
5
6
7
8
DRAWN
CHECKED
QA
MFG
APPROVED
13/0/2016
TITLE
Knee Model (1st Iteration)
University of California, Santa Cruz
SIZE
D
DWG NO
KG-0001
REV
1
SCALE
Sheet 1 of 1
101.60
143.68
88.90
508.00
50.80
118.61
119.81
508.00
127.00
73.7°
143.1°
88.90
135.0°
135.0°
90.0°

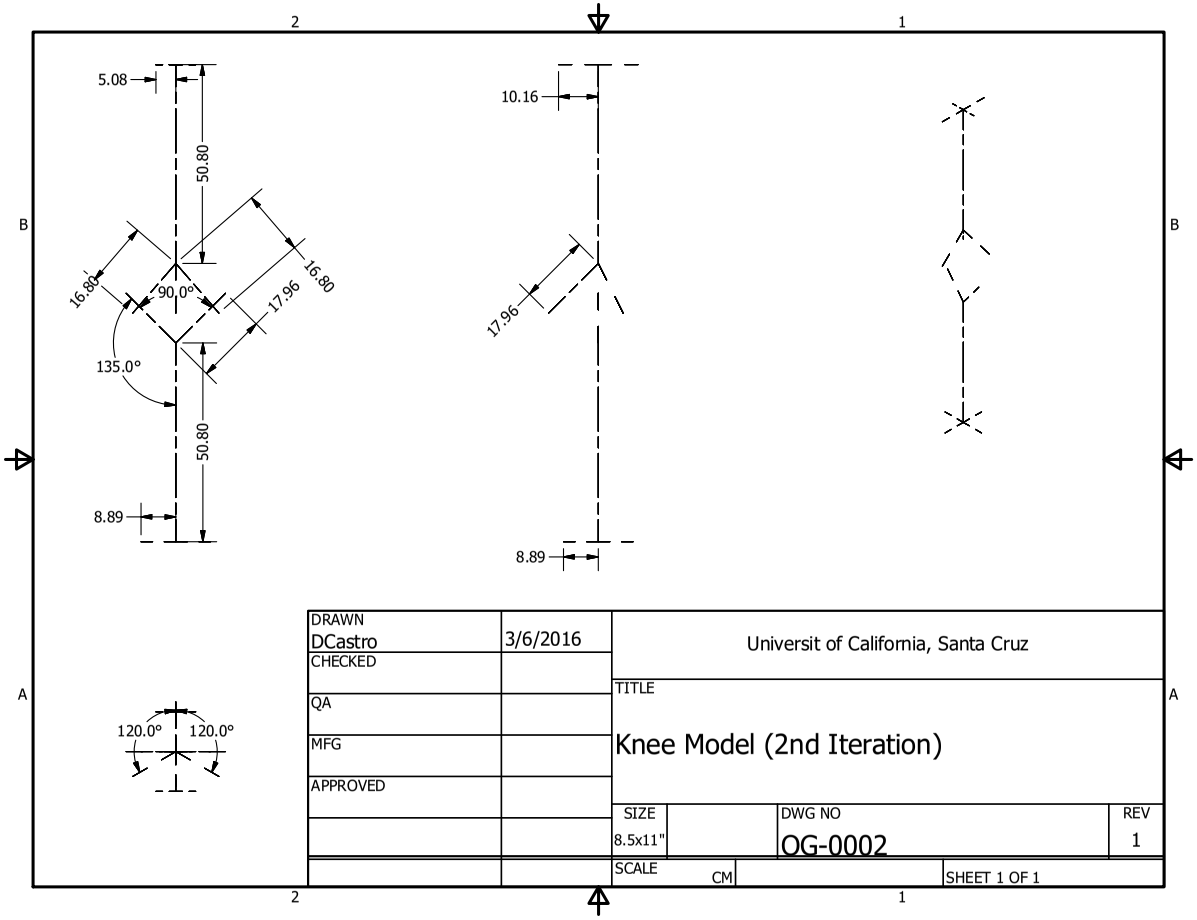
5.08
50.80
16.80
90.0°
17.96
16.80
135.0°
50.80
8.89
10.16
17.96
8.89
120.0°
120.0°
DRAWN
DCastro
3/6/2016
CHECKED
QA
MFG
APPROVED
Universit of California, Santa Cruz
TITLE
Knee Model (2nd Iteration)
SIZE
8.5x11"
DWG NO
OG-0002
REV
1
SCALE
CM
SHEET 1 OF 1

Bibliography

[1] Gage BE, McIlvain NM, Collins CL, Fields SK, Dawn Comstock R. Epidemiology of 6.6 million knee injuries presenting to United States emergency departments from 1999 through 2008. Acad Emerg Med 2012;19:37885.

[2] Simon TD, Bublitz C,Hambidge SJ. Emergency department visits among pediatric patients for sports-related injury: basic epidemiology and impact of race/ethnicity and insurance status. Pediatr Emerg Care. 2006;22:30915.

[3] Yang J, Marshall SW,Bowling JM, Runyan CW,Mueller FO, Lewis MA. Use of discretionary protective equipment and rate of lower extremity injury in high school athletes. Am J Epidemiol. 2005;161:5119.

[4] S.M. Levin, D.C. Martin, Biotensegrity: the mechanics of fascia, R. Schleip, L. Chaitow, T.W. Findley, P. Huijing (Eds.), Fascia the Tensional Network of the Human Body. The Science and Clinical Applications in Manual and Movement Therapy, Elsevier, Edinburgh (2012), pp. 137142

[5] Levin, Stephen M. "Continuous Tension, Discontinuous Compression." A Model for

Biomechanical Support of the Body. Online verfgbar unter http://www. biotensegrity. com/, zuletzt geprft am 5 (1980): 2007.

[6] Gmez-Juregui, V (2010). Tensegrity Structures and their Application to Architecture. Servicio de Publicaciones Universidad de Cantabria, p.19. ISBN 8481025755.

[7] About Intension Designs Ltd. and Bio-Tensegrity, accessed on June 8th, 2015 (http://www.intensiondesigns.com/contact.html)

[8] Structure & Function of the Knee, access on May 27th, 2015 (http://www.mccc.edu/ behrensb/documents/StrucKneebjb.pdf)

[9] Type of Joints, accessed on January 1st, 2017 (http://www.preventdisease.com/fundament/articles/types_of_joints.shtml)

[10] Asano Yuki, Biomimetic design of musculoskeletal humanoid knee joint with patella and screw-home mechanism, Robotics and Biomimetics(ROBIO).

[11] Haegele and Martin and et al, Musculoskeletal Robots and Wearable Devices on the Basis of Cable-driven Actuators, Soft Robotics, Springer Berlin Heidelberg, pg. 42-53, 2015

[12] NASA, NASA Tenesgrity Robotics Toolkit, (http://www.http://ti.arc.nasa.gov/tech/asr/intelligent-robotics/tensegrity/NTRT/)

[13] Bruce, J. and Sabelhaus, A. and Chen, Y. and Lu, D. and Morse, K. and Milam, S. and SunSpiral, V., SUPERball: Exploring tensegrities for planetary probes, Inter-

national Symposium on Artificial Intelligence, Robotics and Automation in Space (i-SAIRAS), Volume 12, 2014

[14] Lawson, B. E. and Mitchell, J. and Truex, D. and Shultz, A., A Robotic Leg Prosthesis: Design, Control, and Implementation, Robotics and Automation Magazine, IEEE, Volume 21, pg. 70-81, 2014

[15] Lessard, Steven, Dennis Castro, William Asper, Shaurya Deep Chopra, Leya Breanna Baltaxe-Admony, Mircea Teodorescu, Vytas SunSpiral, and Adrian Agogino. "A Bio-Inspired Tensegrity Manipulator with Multi-DOF, Structurally Compliant Joints." arXiv preprint arXiv:1604.08667, 2016.

[16] Lessard, Steven, Jonathan Bruce, Erik Jung, Mircea Teodorescu, Vytas SunSpiral, and Adrian Agogino. "A light-weight, multi-axis compliant tensegrity joint." arXiv preprint arXiv:1510.07595, 2015.

[17] Baltaxe-Admony, Leya Breanna, Ash S. Robbins, Erik A. Jung, Steven Lessard, Mircea Teodorescu, Vytas SunSpiral, and Adrian Agogino. "Simulating the Human Shoulder through Active Tensegrity Structures." In ASME 2016 International Design Engineering Technical Conferences and Computers and Information in Engineering Conference, pp. V006T09A027-V006T09A027. American Society of Mechanical Engineers, 2016.

[18] Yokoi, Kazuhito, Fumio Kanehiro, Kenji Kaneko, Kiyoshi Fujiwara, Shuji Kajita, and Hirohisa Hirukawa. "A honda humanoid robot controlled by aist software." In

Proc. of the IEEE-RAS International Conference on Humanoid Robots, pp. 259-264. 2001.

[19] Park, Ill-Woo, Jung-Yup Kim, Jungho Lee, and Jun-Ho Oh. "Mechanical design of humanoid robot platform KHR-3 (KAIST humanoid robot 3: HUBO)." In Humanoid Robots, 2005 5th IEEE-RAS International Conference on, pp. 321-326. IEEE, 2005.

[20] Modulus of Elasticity or Youngs Modulus and Tensile Modulus for common Materials, accessed on December 1th, 2016, (http://www.engineeringtoolbox.com/young-modulus-d_417.html)

[21] Densities of Wood Species, accessed on December 1th, 2016, (http://www.engineeringtoolbox.com/wood-density-d_40.html)

[22] Wood Hardness, accessed on December 1th, 2016, (http://www.engineeringtoolbox.com/wood-hardness-d_559.html)

[23] Bartel, Donald L., and Dwight T. Davy. Orthopaedic biomechanics: mechanics and design in musculoskeletal systems. Prentice Hall, pg. 315, 2006.

[24] Hefzy, M. S., B. P. Kelly, T. D. Cooke, A. M. Al-Baddah, and L. Harrison. "Knee kinematics in-vivo of kneeling in deep flexion examined by bi-planar radiographs." Biomedical sciences instrumentation 33 (1996): 453-458.